THE UNIVERSITY OF NEW SOUTH WALES

SCHOOL OF MECHANICAL AND MANUFACTURING ENGINEERING

Natural Frequency Statistics of an Uncertain Plate

Surasak Patarabunditkul

3156945

Bachelor of Engineering (Mechatronic)

June 2009

Supervisor Dr Nathan Kinkaid

Abstract

This thesis is concerned about designing an uncertain dynamic system to observe the effect of uncertainty to the system which has perfect symmetry. The steel circular plate was selected and designed to be able to stimulate a set of different configuration of uncertainty. The choice of equipment and procedure and frequency range of interest has been selected. The qualitative measure of the will be the natural frequency statistics using two statistical measures; the statistical overlap factor and the probability density function of the spacing between successive natural frequencies. The statistical overlap factor is the variation in a natural frequency from its mean value measured across the set of system with different uncertainty. The probability density function of natural frequency spacing was applied to each individual to observe the Rayleigh distribution where it is a feature of the universality exhibited by structures with uncertain. The effect will be monitored to see if it is greater or lower as the frequency is getting higher. The outcome was concluded that the effect of material stiffness permutation using aluminium bar was neglectable or very low. The unexpected effect of negative mass which holes initially drilled to fix the aluminium bar to the steel plate was very dominant. The study also incorporated simulation software to generate the perfect system without any negative mass and other material variation. The two resulted were compared, simulation result verified the neglectable effect of aluminium bar. The simulation study was continued to detect at what stiffness the system will be random enough to produce Rayleigh distribution.

Statement of Originality

I hereby declare that this document contains no materials previously submitted for any degree or other award at UNSW or any other institution. It is my belief that all work in this thesis is entirely my own work, except where stated and otherwise referenced, is my own original work. I consent for this thesis to be available for academics and students within the University for loan and database access.

Signature

Date

Acknowledgement

Firstly and importantly, I would like to thanks Dr Nathan Kinkaid my supervisor who gave me a chance to do this thesis. I am also appreciating his guidance, kindness and expertise throughout the project whenever I needed.

Secondly, I thank Mr Russell Overhall for his help with setting up the experimental components of my thesis. His practical assistances and comments from his experience were valuable.

I need to thanks my family members for their support and motivation to encourage me to complete this thesis. I also specially mention Arunothai Ekkhosit with her help in ANSYS and support, always.

Lastly I cannot forget to thanks my friends Charles Sithu, Dany Pradhana and Eric Poon for their comments and helps.

Thank you

Table of content

List of Figure

List of Table

List of symbol

b	Parameter of Rayleigh Probability density function
μ	Mean of sample
$N(i)$	Ordered statistic median
G	Inverse of the cumulative distribution function
$U(i)$	Uniform ordered statistic median
S	Statistical overlap factor
σ	Standard deviation
λ^2	Frequency parameter
∇^2	Laplacian operator
W	Position co-ordinate function
$W_{m,n}$	Plate displacement
D	Flexural rigidity
H_1	FRF estimator
Φ	Phase angle
m	Mass
c	Damping coefficient

k	Stiffness
F	Force
A	Acceleration
V	Velocity
X	Linear displacement
Pa	Pascal (N/m^2)

1. Introduction

Vibrations are a part of human everyday life in one form or another. Vibrations have both a great effect and devastating effect on human society. Since ancient times humans have experienced the impact of vibration both manmade and natural. An earthquake is an example of devastating consequence of vibration. However, benefits from application of vibration are diverse in both scientific and non-scientific fields. Music was an early application of vibration, stringed music instrument appears on the wall of Egyptian tomb which can be dated back to about 3000 B.C. [1]. Today, vibration analysis contributes toward many fields such as mechanical and civil engineering and medicine.

Vibrations, however, can be passively generated and normally are undesired. Rotating imbalance in rotational machinery such as gearboxes or motors can create this unwanted vibration. Oscillation that is a consequence from operation of machine can create excessive noise or fatigue in a machine and result in catastrophic failure.

These factors, good and bad, have motivated humans to study vibrations to better understand, benefit and prevent their undesirable consequences. From an engineering point of view vibrations are an important factor in the design phase due to undesirables such as noise and catastrophic factors such as vibration induced fatigue and wear.

One of aspect of vibration analysis that has been of great interest is a mathematical model for a particular system. The analysis of the response of a vibrational system relies on constructing a mathematical model or an equation of motion in order to calculate natural frequencies and mode shapes. For a complex system that is difficult to model, approximations use various modeling techniques such as finite element analysis (FEA). Finite element analysis cannot accurately predict response of a system with inherent randomness but rather an analysis would yield an approximation of the response of the ensemble member whose properties most closely match that of the finite element model [2].

Every engineering structure and machine possesses uncertainty. The uncertainty concerned in this thesis is the variation in material properties such as mass and stiffness. The response of any system with uncertainty will differ from the response of a system model. The level of variation of the response will depend on the degree of uncertainty. At low frequencies, the effect is often negligible, but as the frequency increases, the effect becomes more apparent.

In this thesis, a steel circular plate will be the system of interest. The uncertainty will be introduced by fixing a number of aluminium bars on to the plate. As a range of similar uncertain systems will be studied, a series of uncertain plate can be achieved by rearranging the orientation of each aluminium bar.

The study of natural frequency of an uncertain plate will be using the statistic to observe the effect of uncertainty on the system at a range of frequency. The two main statistic measurements are the statistical overlap factor and the probability density function of the spacing between successive natural frequencies.

1.1 Literature Review

In 1973, Chen and Soroka [3] study impulse response of a simple dynamic system. The equation of motion is modelled with natural frequency is being random variable. The natural frequency modelled as a sum of mean frequency and product of perturbation parameter and perturbation with zero mean. They solve the ordinary differential equation with random coefficient by Samuels and Eringen. The result was plotted in term of magnitude of standard deviation. They remarked the amplitude of the standard deviation to increase as the mean frequency increase and dampened out after it reached certain level. Furthermore, the value of standard deviation diminished as the mean natural frequency of the system increased. The result of plotting indicates that a system at low frequency, the uncertainty in natural frequency can be ignored in predicting the system response where as the system with high natural frequency the effect of uncertainty to the frequency response is significant.

Leissa and Narita [4] determined a range of natural frequency of simply supported circular plate. The motivation was from the extensive investigation of free and clamped boundary condition but not simply support. The results shown include Poisson's ratio from 0 to 0.5 in 0.1 steps. The presented work covers all value of nodal diameters 'n' and nodal circles 's' and which 'n' plus 's' is less than or equal to 10. The mode shape presented will be use as reference to determine the location of the accelerometer and excitation point.

S.McWilliam et al [5]. investigated the natural frequency of rings attached with random mass. The interested arrangements were

(a) random harmonic variations in the mass per unit length around the circumference of the ring

(b) the attachment of random point masses at random locations on the ring

(c) the attachment of random point masses at uniformly spaced positions on the ring

The frequency spacing's were found by analytical expression rather than by experimental results. The Rayleigh-Ritz method was used in the analysis with assumption that the mode shape of the imperfect ring was the same as the perfect ring. The results have shown that for case (a) the frequency spacing distribution demonstrated Rayleigh distribution. The remarkable observation for case (b) was the distribution tending to Rayleigh as the degree of randomness was increased, in this case the number of point mass increased. Case (c) the distribution was depending on the particular modes that taken into account and number of point mass added to the system. In a perfectly axisymmetric body the vibration modes for a given nodal configuration occur in degenerate pairs which (a) have equal natural frequencies, (b) are spatially orthogonal and (c) have indeterminate angular location around the axis of symmetry [6]. If any imperfection were to be introduced into such perfect system, the initially equal natural frequency pair would be split. It was found that the magnitude of the frequency split was a function of the magnitude of the imperfection and the angular location of the modes which determined by the spatial distribution of the imperfection.

For an isotropic circular plate with constant thickness and free edges, its fundamental vibration mode took the form of a twisting mode with 2 nodal diameters. Wang [7] presented that with certain modification, such a fundamental modes with 2 nodal diameters become axissymetric mode shape. The proposed method were the adding outer rim to the circular plate with material with lager Young's modulus or using the same material but larger in thickness.

Lin and Lim[8] studied the rectangular plate with arbitrary mass and stiffness modification. Plate receptances were derived based on mode superposition and then used to calculate the receptances of the modified plate. Natural frequencies and mode shapes of the modified plate were identified by analysing the receptance data based on the concept of modal analysis. They proposed a method which proved to be effective and accurate to predict natural frequencies and mode shapes of such a plate mentioned above. There were 4 scenarios considered

(a) mass
(b) mass and stiffness
(c) mass, stiffness and damping
(d) mass, stiffness and damping at both translation and rotational.

Here, the result is to be concerned rather the methodology provided. The outcomes were presented for the first 7 natural frequencies of the dynamic system. The notable result is the variation in natural frequencies from original system was most affected by the mass modification alone rather other combination of different modification.

Lucus [9] has done extensive research on dynamic systems with a range of permutation. The experiments were conduct to study the effect of the specific type of permutation, namely stiffness and mass, on the natural frequency of the system. The result is studied statically. The 2 measures that were used to measure the result were successive natural frequency spacing which quantified by histogram and statistical overlap factor. The part of research has been thoroughly reviewed which considered to be related to this thesis are point mass permutation, stiffness permutation created by spring and the combination of both. The dynamic system which these variations exist was an aluminium rectangular plate of size 899 mm in length, 600 mm in width and thickness of 2 mm. The experiment were conduct by

(a) increase the number variation on the system which were of the same degree of randomness

(b) increase number variation applied on the system but keeping the total of degree of randomness constant

These rules were both applied to mass variation, stiffness variation and the combination of both. The effect of mass uncertainty revealed that the greater the numbers of uncertainty the greater of the effect. The effect was seen by the trend of natural frequency splitting tend towards Rayleigh distribution as the number of randomness increased. It was also noted that the effect of mass permutation increased as the frequency increased, but it would become saturated at a certain frequency. This was pointed out by statistical overlap factor graph where it increased with frequency but level off at a specific point with the bigger the number of randomness the higher overlap factor curve level off. The frequency at the curve started to become saturated was relatively the same regardless of number of variation. The mean spacing also presented a relatively constant behaviour across the ensemble as well as each member. The inertia of each mass was accounted for one of the cause of variation.

It was confirmed in the (b) part experiment that the number of permutation applied would determine the variation in system response. The result indicated that, even though, the degree of randomness was constant. The histogram of natural frequency spacing was nearest to Rayleigh distribution when the number of mass was greatest although each added mass was less. It was further emphasised when only 1 mass, whose mass was equal to total mass of different configuration applied, showed an almost straight line in statistical overlap factor curve.

The local stiffness variation, however, showed inverse relationship in statistical overlap factor. The spring was attached to the plate and ground. The curve deceased as the frequency got higher and tended toward 0. It was interpreted that the effect of the spring was getting lower at high frequency. When the rule (b) applied, the closest match was not from the most number of springs.

2. Vibration Basic

Vibration is a motion of a particle that moving back and forth about equilibrium position. The motion is cyclic. Vibration can be distinguished into 2 types, free and force. Free vibration is when the system is oscillating in the absence of external force. It will vibrate at its one or more natural frequencies. The forced vibration system will vibrate at the frequency of the applied force. When the applied exciting frequency is coincide with one of the system natural frequency, the response amplitude become large and, sometime depending on system, large enough to cause damage to surrounding or the system itself. It is known as resonance when the exciting force is at system natural frequency. Resonance contributes to the failure of structure such as bridge, turbine and machine.

The vibrating system generally includes a mean for storing potential energy (e.g. spring) and a mean for storing kinetic energy (e.g. mass) [10]. The vibration of a system involves transferring back and forth between potential and kinetic energy. The system may also be subjected to energy dissipating or resistance source known as damping. Since the system is losing energy during the motion, free vibration will decrease and eventually become at rest. However the forced vibration can remain at the exciting frequency with requirement of energy to be supplied. The system with energy dissipating source is called damped system. The damping of the system also influences the natural frequency of system.

The number of independent coordinate necessary to describe the motion of a system is called the degree of freedom of the system [11]. A system with ‘n’ degrees of freedom will have ‘n’ natural frequency.

The system can be further categorised into linear and nonlinear vibration. When the components of the system, spring and mass for example, have linear behaviour, it is linear vibration. The principle of superstition holds in linear system whereas the nonlinear does not. All system, however, normally behaves nonlinearly at high amplitude.

The most basic configuration of vibrating system is system with one degree of freedom, which consist of a block of weight

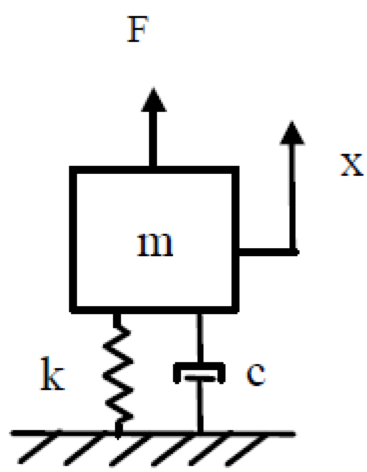

Figure 2.1 – Single degree of freedom system

Where

m is the mass

x is the displacement

k is stiffness

c is the damping coefficient

F is the force

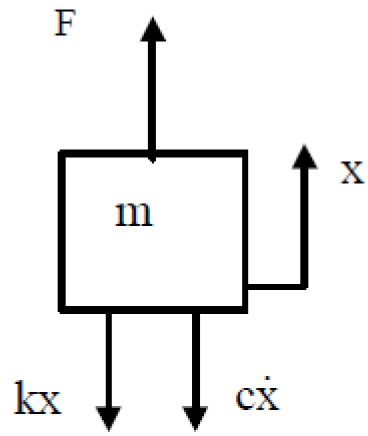

Figure 2.2 – Free body diagram of single degree of freedom system

Equation of motion of the single degree of freedom is

$$\sum F = m\ddot{x} \tag{2.1}$$

$$F - kx - c\dot{x} = m\ddot{x} \tag{2.2}$$

For modal model, the external force is not taken into account or it is free vibration therefore

$$m\ddot{x} + c\dot{x} + kx = 0 \tag{2.3}$$

The general solution to a SDOF system in free vibration is given by an exponentially decaying sine function as follows

$$x(t) = Ae^{-\omega_n \xi t} \sin(\omega_d t + \phi) \tag{2.4}$$

Where

A is the amplitude

t is the time

ϕ is the phase angle

ξ is the damping ratio

ω_n is the system natural frequency

ω_d is the damped natural frequency given by $\omega_d = \omega_n \sqrt{1-\xi^2}$ (2.5)

If the single degree of freedom systems are subject to force such as harmonic force the equation of motion becomes

$$m\ddot{x} + c\dot{x} + kx = F_0 \sin \omega t \qquad (2.6)$$

Where

F_0 is the maximum force amplitude

ω is the frequency of harmonic force

The general solution to equation (2.6) is

$$x(t) = \frac{F_0}{k} \frac{\sin(\omega t - \phi)}{\sqrt{\left(1-\left(\frac{\omega}{\omega_n}\right)^2\right)^2 + \left(2\xi \frac{\omega}{\omega_n}\right)^2}} \qquad (2.7)$$

From equation (2.7), it can be seen that the maximum displacement will occur when exciting frequency ω is near natural frequency ω_n. The maximum displacement is also influenced by the damping of the system, the higher the damping, the lower the maximum displacement.

2.1 Modal testing

The study of vibration response of a structure is to be to understand its nature and be able to control it. There are 2 general types of tests, signal analysis and system analysis [12]. The signal analysis is the process of determining the response of a system due to unknown excitation which generally operational force, in another word when it is in real operation. The system analysis involves determining the inherent properties of the system by stimulating the system with known force and then study it response. This is generally made under controlled condition and yield more accurate and detail information than the first type. It consists of data acquisition and analysis of data, the data is from testing of structure of interest where the analysis yields mathematical description of their dynamic behaviour. It is known as modal testing. The ultimate result of modal testing is extraction of modal parameter namely; modal frequency, modal damping and modal shape. They are used to constructing mathematical dynamic model.

The applications of the acquired model are vast but the most common application is the measure of vibration mode to verify with theoretical model that has been develop earlier. This is to ensure the accuracy of theoretical model before use.

2.1.1 Measurement method

The quality of the obtained data depends on the acquisition method to ensure that data analysis will yield accurate information. There are 3 areas in which need particular attention to make sure the quality of measure data is high [13].

2.1.1.1. The mechanical aspect of the supporting and exciting structure

There are normally 3 options; free or unrestrained, grounded and in situ. With free condition, the structure will exhibit rigid body modes which are determined completely by its mass and inertia properties and will be no bending or flexing at all. It is normally setting the test structure to be completely free in real life. Free is usually achieved by suspend the structure to be tested with very soft spring or elastic band. The point of suspend should be put as close as possible to nodal point of the mode in interest. If possible, the suspend direction is put normal to primary direction of vibration. The structure of interest that is grounded will be rigidly cramped. It is crucial to provide the foundation that is sufficiently rigid. The confirmation is to check the mobility of the support over the range of testing frequency and compare whether it is relatively low when compare to the structure at the point of contact.

It is usually that the free support will be the best option of supporting type as no extraordinary attention requires to verify the ground support achieves grounded condition but in case where structure is large, the free support is almost impossible.

The condition of the normal operation of test structure can influence the type of support chosen, if it is normally grounded the supporting obviously should be grounded which is close to those of the operational structure. In situ means the structure will be connected to some other structure or component non-rigidly.

2.1.1.2 The correct transducer of the quantities to be measured

The transducer is essential part as it is the component that will input and measure the data such as force, acceleration and velocity. The choices of transducer depend on the range of data to be read and the type of structure that undergo testing. The response measurement of motion parameter, force and acceleration, often use piezoelectric accelerometer due to it number of advantage. It has good linearity, low weight, broad dynamic range, wide frequency rage, low transverse sensitivity and applicable for number of mounting method. Input force measurement is usually done by piezoelectric force transducer

One problem needs to be taken into account is the influence of the transducer to the test structure. Incorrect use of transducer can contribute to major error. Using a large transducer to measure response on a flexible plate will create local loading in the area can lead to inaccurate response. This will also result in increase in stiffness or damping which will lower the measured natural frequency of the system. Therefore, where possible, a light transducer is preferred especially when testing in high frequency.

The transducer mounting method is important as transducer itself and need to be carefully selected. There are range of mountings can be chosen from. The available are steel stud, bee wax, cement stud, thin tape, thick tape and magnet. For optimal performance the steel stud is the first choice but it not, however, always convenience and applicable in small or flexible structure. The more convenience way yet still giving good result is applying bee way at the base of transducer and firmly pressed onto structure. Although the narrower frequency range but without modification of the structure as in steel stud case, it is one of popular choice of mounting technique.

2.1.1.3. The signal processing which is appropriate to the type of test

The choice of function used in the processing need to be corresponded to the type of test being performed

2.1.2 Excitation

There are 2 excitation types; contacting and non-contacting [13]. The contacting exciter will be attached to test structure and remain there throughout the vibration period. The second type of excitation, the exciter can always be out of contact or in contact for a short period of time to excite the test structure. Examples of attached exciters are electromagnetic shaker, electrohydraulic shaker and eccentric rotating masses. Examples of non-attached exciters are hammers and suspended cable to produce snap back.

2.2 Fast Fourier Transform

Fourier transform is initially used to convert a continuous function that is functions which are defined at all values of the time ‘t’, from time domain into frequency domain.

Digital signal processing involves discrete signals which are from the sample of interested signal rather than continuous signals. The conversion process is then needed what is called Discrete Fourier Transform or DFT, it is the modification of Fourier Transform.

The output or the result of the DFT is a set of sine and cosine coefficients. Reconstruction of the original wave signal is done superimpose the product of each obtained coefficients with appropriate sine or cosine waves with appropriate frequency. The sine or cosines are the frequency components of the original wave where the coefficient is the amplitude contents. The spectrum is complex quantity.

DFT is a straight forward calculation but it, however, requires numerous steps. It needs to perform N^2 calculation for DTF where N is the number of sample [14].

Numerical algorithm developed by Cooley and Tukey[15] called Fast Fourier Transform allows DFT to perform with significant reduction in calculation steps. This is presented in “An algorithm for the machine calculation of complex Fourier series” published in 1965.

The process of determining the amplitudes of all the frequency components of a signal is known as spectrum analysis. The frequency versus amplitude is called the spectrum of the signal. The term that will come across is autospectrum and cross spectrum. The autospectum is obtained by multiplying a spectrum by its complex conjugate and by averaging a number of independent products while cross spectrum is from the multiplication of one spectrum and complex conjugate of different spectrum. The cross spectrum is complex where it phase is the phase shift between input and output.

2.3 Frequency Response Function

Frequency response function is a transfer function $H(\omega)$ given by [16]

$$H(\omega) = \frac{X(\omega)}{F(\omega)} \tag{2.8}$$

Where

$F(\omega)$ is input force spectrum

$X(\omega)$ is output spectrum

It is complex function which contains both magnitude and phase. The output spectrum can be of displacement, velocity or acceleration, which reflect the name of frequency response function.

Displacement / Force	Velocity / Force	Acceleration / Force
Admittance Compliance Receptance	Mobility	Accelerance Inertance

Table 2.1 Type of Frequency Response Function

The frequency response will be applied to single degree of freedom as an example

From equation of motion

$$F = m\ddot{x} + c\dot{x} + kx$$

$$\frac{F}{m} = \ddot{x} + \frac{c}{m}\dot{x} + \frac{k}{m}x \tag{2.9}$$

$$\frac{c}{m} = 2\xi\omega_n \tag{2.10}$$

$$\frac{k}{m} = \omega_n^2 \tag{2.11}$$

Where

ω_n is undamped natural frequency

ξ is damping ratio

Substitute equation (2.10) and (2.11) into equation (2.9)

$$\frac{F}{k}\omega_n^2 = \ddot{x} + 2\xi\omega_n\dot{x} + \omega_n^2 x \tag{2.12}$$

The final Fourier transformation is given by [5]

$$\frac{X(\omega)}{F(\omega)} = \left[\frac{1}{k}\right]\left[\frac{\omega_n^2}{\omega_n^2 - \omega^2 + j(2\xi\omega\omega_n)}\right] \tag{2.13}$$

This has magnitude

$$\left|\frac{X(\omega)}{F(\omega)}\right| = \left[\frac{1}{k}\right]\left[\frac{\omega_n^2}{\sqrt{\left(\omega_n^2 - \omega^2\right)^2 + (2\xi\omega\omega_n)^2}}\right] \tag{2.14}$$

And phase

$$\Phi = \arctan\left[\frac{2\xi\omega\omega_n}{\omega_n^2 - \omega^2}\right] \tag{2.15}$$

The similar analysis can be done using Fourier transform to obtain mobility and accelerance

Mobility is

$$\frac{V(\omega)}{F(\omega)} = \left[\frac{1}{k}\right]\left[\frac{j\omega\omega_n^2}{\omega_n^2 - \omega^2 + j(2\xi\omega\omega_n)}\right] \tag{2.16}$$

The magnitude is

$$\left|\frac{V(\omega)}{F(\omega)}\right| = \left[\frac{1}{k}\right]\left[\frac{\omega\omega_n^2}{\sqrt{\left(\omega_n^2-\omega^2\right)^2+(2\xi\omega\omega_n)^2}}\right] \tag{2.17}$$

And the phase is

$$\Phi = \arctan\left[\frac{-\omega_n^2+\omega^2}{2\xi\omega_n}\right] \tag{2.18}$$

Accelerance has the form

$$\frac{A(\omega)}{F(\omega)} = \left[\frac{1}{k}\right]\left[\frac{-\omega^2\omega_n^2}{\omega_n^2-\omega^2+j(2\xi\omega\omega_n)}\right] \tag{2.19}$$

Where its magnitude is

$$\left|\frac{A(\omega)}{F(\omega)}\right| = \left[\frac{1}{k}\right]\left[\frac{-\omega^2\omega_n^2}{\sqrt{\left(\omega_n^2-\omega^2\right)^2+(2\xi\omega\omega_n)^2}}\right] \tag{2.20}$$

And phase is

$$\Phi = -\pi + \arctan\left[\frac{2\xi\omega_n}{\omega_n^2-\omega^2}\right] \tag{2.21}$$

Since the measurement process experience noise which might come from surrounding environment or instrument itself. Engineering measurement often involves averaging process which the same in this case. The averaging minimise the error causing by noise in reading. The approach is to use the principle of least square method which resulting in FRF estimator

$$\hat{H} = \frac{\sum F^* X}{\sum F^* F} \tag{2.22}$$

This estimator is called H_1 and is equal to ratio of cross spectrum of response and force over autospectrum of force.

$$H_1(\omega) = \frac{G_{FX}(\omega)}{G_{FF}(\omega)} \tag{2.23}$$

2.4 Plate Theory

The study of plate vibration was inspired by the successful of Euler's membrane equation. Euler [17] derived equations for the vibration of rectangular membranes, but however it was only correct for the uniform tension case. He considered the rectangular membrane as a superstition of two set of strings laid in perpendicular direction.

With the German physicist, Chladni, is accounted for the first to have a serious study of plate vibration. The experiment was on observing the nodal pattern of vibration on rectangular plate. Sand was spread on to interested plate where it was let free to vibrate, after the plate came to rest the sand accumulated along nodal line.

The first numerical method was developed by Germain, where she proposed the differential equation of transverse deformation of plate by means of calculus of variation.

It, however, was corrected by Lagrange for neglecting the strain energy due to warping of the plate midplane [18].

The plate theory was then further improve by Kirchhoff which included bending and stretching effect. Kirchhoff plate theory is referred as Classical Plate Theory.

Mildlin later proposed that the effect of rotatory inertia and transverse shear strain was significant and cannot be omitted as in the Classical Plate Theory. The modified plate equation of motion is known as Shear Deformable Plate Theory.

Recent refinement on plate theory was proposed by Reddy, his third order shear deformation theory give zero shear stress condition at free surface is satisfied.

2.4.1 Fundamental Equation of Classical Plate Theory

The displacement w of plate given by Leissa [19] is

$$D\nabla^4 w + \rho \frac{\partial^2 w}{\partial t^2} = 0 \tag{2.24}$$

Where D is the flexural rigidity given by

$$D = \frac{Eh^3}{12(1-v^2)} \tag{2.25}$$

E is Young's modulus

h is the plate thickness

v is Poisson's ratio

ρ is mass density per unit area

t is time

$\nabla^4 = \nabla^2\nabla^2$

∇^2 is the Laplacian operator

When the free vibration is assumed, the motion is expressed by

$$w = W\cos\omega t \tag{2.26}$$

ω is circular frequency in radian per unit time

W is a function only of the position coordinate

Substitute equation (2.26) into (2.24)

$$(\nabla^4 - k^4)W = 0 \tag{2.27}$$

$$k^4 = \frac{\rho\omega^2}{D} \tag{2.28}$$

$(\nabla^4 - k^4)W = 0$ can be rewritten as $(\nabla^2 - k^2)(\nabla^2 - k^2)W = 0$

The solutions to linear differential equation above are

$$\nabla^2 W + k^2 W = 0$$

$$\nabla^2 W - k^2 W = 0 \tag{2.29}$$

In the case of plate supported by a massless elastic medium equation (2.24) become

$$D\nabla^4 w + Kw + \rho \frac{\partial^2 w}{\partial t^2} = 0 \qquad (2.30)$$

K is stiffness of the foundation in unit of force per unit length of defection per unit area of contact

Assuming the deflection form (2.26) and substituting into equation (2.30)

$$k^4 = \frac{\rho\omega^2 - K}{D} \qquad (2.31)$$

Circular Plate

The Laplacian operator expressed in circular coordinate is

$$\nabla^2 = \frac{\partial^2}{\partial r^2} + \frac{1}{r}\frac{\partial}{\partial r} + \frac{1}{r^2}\frac{\partial^2}{\partial \theta^2} \qquad (2.32)$$

When Fourier component in θ are assumed

$$W(r,\theta) = \sum_{n=0}^{\infty} W_n(r)\cos n\theta + \sum_{n=1}^{\infty} W^*{}_n(r)\sin n\theta \qquad (2.33)$$

Substitute equation (2.33) into equation (2.29)

$$\frac{d^2 W_{n1}}{dr^2} + \frac{1}{r}\frac{dW_{n1}}{dr} - (\frac{n^2}{r^2} - k^2)W_{n1} = 0$$

$$\frac{d^2 W_{n2}}{dr^2} + \frac{1}{r}\frac{dW_{n2}}{dr} - (\frac{n^2}{r^2} + k^2)W_{n2} = 0 \qquad (2.34)$$

And two identical equation for W^* equations (2.34) are recognised as form of Bessel's equation having solutions

$$W_{n1} = A_n J_n(kr) + B_n Y_n(kr)$$

$$W_{n2} = C_n I_n(kr) + D_n K_n(kr) \tag{2.35}$$

J_n and Y_n are the Bessel function of the first and second kinds

I_n and K_n are modified Bessel function of the first and second kinds

coefficient $A_n\ B_n\ C_n\ D_n$ determine the mode shape and solved for from the boundary condition

The general solution to equation (2.27) in polar coordinate is

$$\begin{aligned} W(r,\theta) = \sum_{n=0}^{\infty}[A_n J_n(kr) + B_n Y_n(kr) + C_n I_n(kr) + D_n K_n(kr)]\cos n\theta + \\ \sum_{n=1}^{\infty}[A_n^* J_n(kr) + B_n^* Y_n(kr) + C_n^* I_n(kr) + D_n^* K_n(kr)]\sin n\theta \end{aligned} \tag{2.36}$$

When the origin of a polar coordinate system is taken to coincide with the centre of the solid circular plate equation (2.36) with assumption, $Y_n(kr)$ and $K_n(kr)$ are discarded to avoid infinite deflection and stresses at r=0, the boundary condition possess symmetry with respected to one or more diameter of the circle then the terms involving $\sin n\theta$ is not needed become

$$W_n = [A_n J_n(kr) + C_n I_n(kr)]\cos n\theta \tag{2.37}$$

n can take on all values from 0 to ∞

The subscription n will correspond to number of nodal diameters

3. Statistic Measure

The statistic descriptors interested in this study of a structure with random properties are the probability density function of natural frequency spacing and statistical overlap factor. Set natural frequency spacing across ensemble of sample are arranged in increasing order then fitted into a probability density function. To measure how well a set of data fit into a distribution function, probability plot is employed.

3.1 Rayleigh Distribution function

Rayleigh probability density function is given by [20]

$$\frac{x}{b^2} e^{\left(\frac{-x^2}{2b^2}\right)} \tag{3.1}$$

Where b is the parameter of Rayleigh Probability density function defined by $\mu\sqrt{\frac{2}{\pi}}$ where μ is the mean of sample

Figure 3.1 illustrates sample Rayleigh distributions, both are Rayleigh distribution but are of different parameter. The wider the distribution, the higher the parameter which it indicates the higher mean of data. As Rayleigh distribution is determined by the parameter which related to mean of data, the mean of the natural frequency spacing obtained experimentally will be used to derive the parameter to generate Rayleigh distribution and compare how well it fit in the distribution.

Figure 3.2 shows a Rayleigh distribution generated by a sample mean which data were sampled randomly and its histogram.

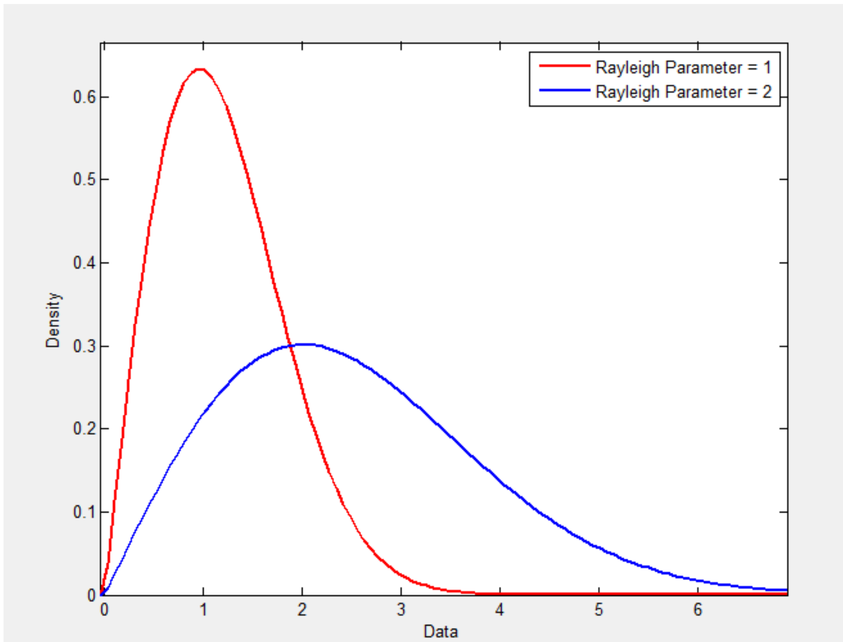

Figure 3.1 – Examples of Rayleigh Distribution

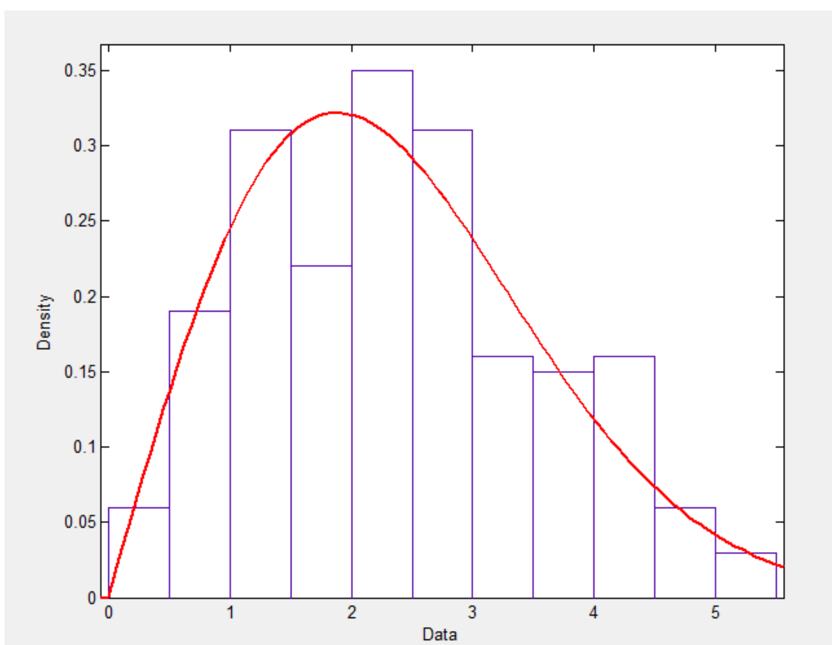

Figure 3.2 – Rayleigh distribution generated from sample mean and its histogram

3.2 Probability plot

Probability plot provides a simple effective means of determine whether a sample of data belong to specified probability distribution [21]. If the ordered samples are plotted against the expected values of the order statistic of standardised distribution, then the result should be linear. If the test data is not from the assumed distribution, the linear pattern will not be observed. The equation is given by

$$N(i) = G(U(i)) \tag{3.2}$$

Where

$N(i)$ are ordered statistic median

G is the inverse of the cumulative distribution function

$U(i)$ are the uniform ordered statistic median defined by

$$U(1) = 1 - U(n) \tag{3.3}$$

$$U(i) = \frac{i - 0.3175}{n + 0.365} \tag{3.4}$$

$$U(n) = 0.5^{\frac{1}{n}} \tag{3.5}$$

The inverse cumulative distribution function is given by [22]

$$s = c\sqrt{-2\ln(1 - U(i))} \tag{3.6}$$

The interested data will be plotted against ordered statistic medians $N(i)$, $N(i)$ will form horizon axis where data in arranged increasing order will form vertical axis.

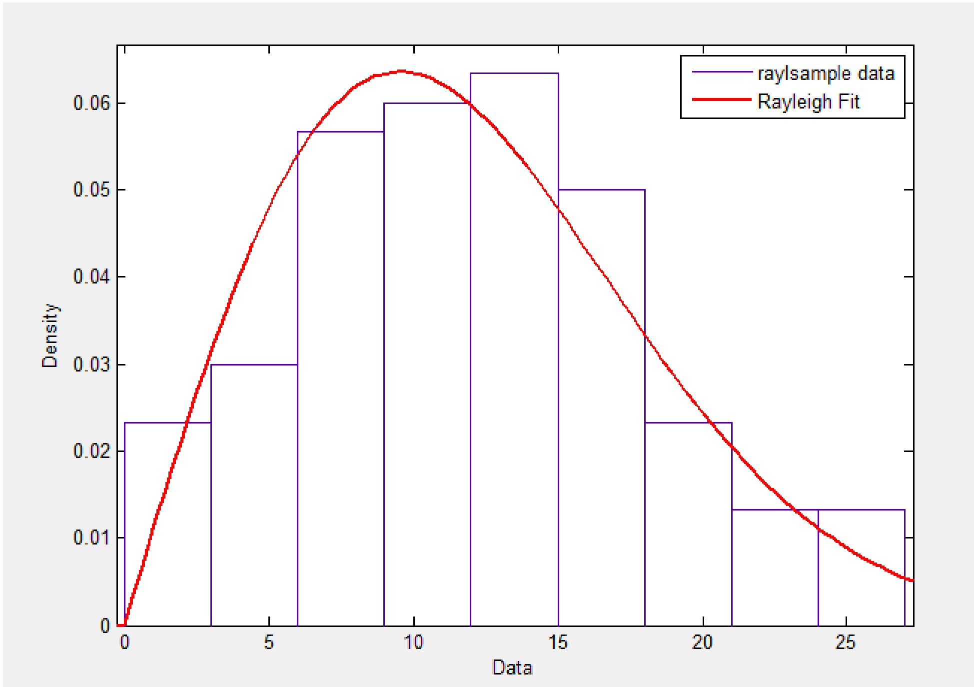

Figure 3.3 – MATLAB randomly sampled data from Rayleigh distribution

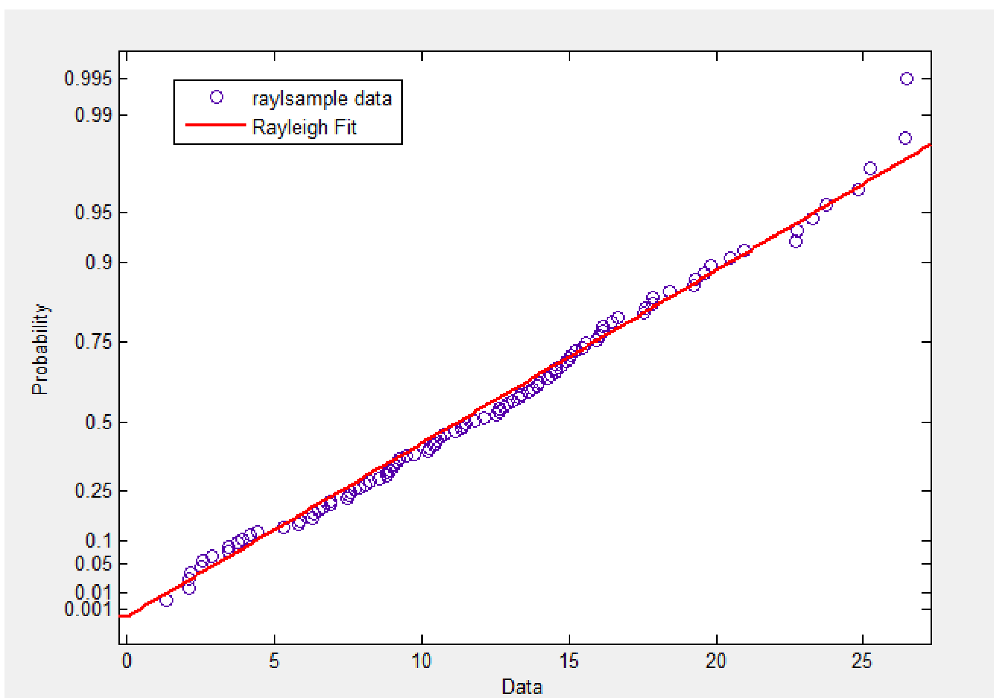

Figure 3.4 – Rayleigh Probability Plot

The 100 sample numbers taken from Rayleigh distribution generated by MATLAB are plotted in figure 3.3, the red line in figure indicate the Rayleigh distribution created by using the mean of the samples. The Rayleigh probability plot of the same samples is shown in figure 3.4, again the red line is a benchmark of perfect Rayleigh distribution. Figure 3.5 shows exponential distribution which was generated by MATLAB, its Rayleigh probability plot is in figure 3.6. The result is obviously does not follow the red straight line, a suggestion for perfect Rayleigh distribution, it can be concluded that the data were not from Rayleigh distribution which is initially known. The data is, however, expected to produce a straight line result in exponential probability plot. Probability plot is a useful statistical technique to quickly check if the set of data are from assumed distribution.

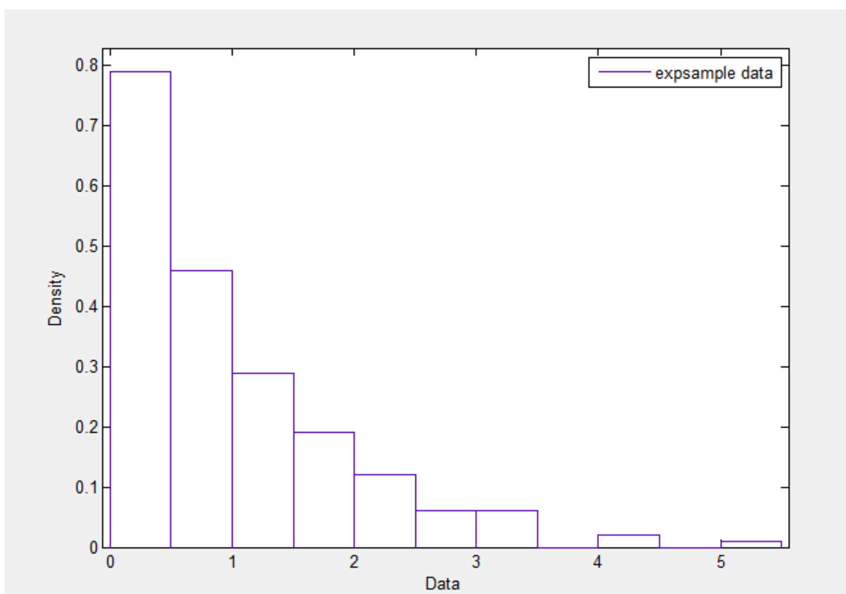

Figure 3.5 – exponential distribution

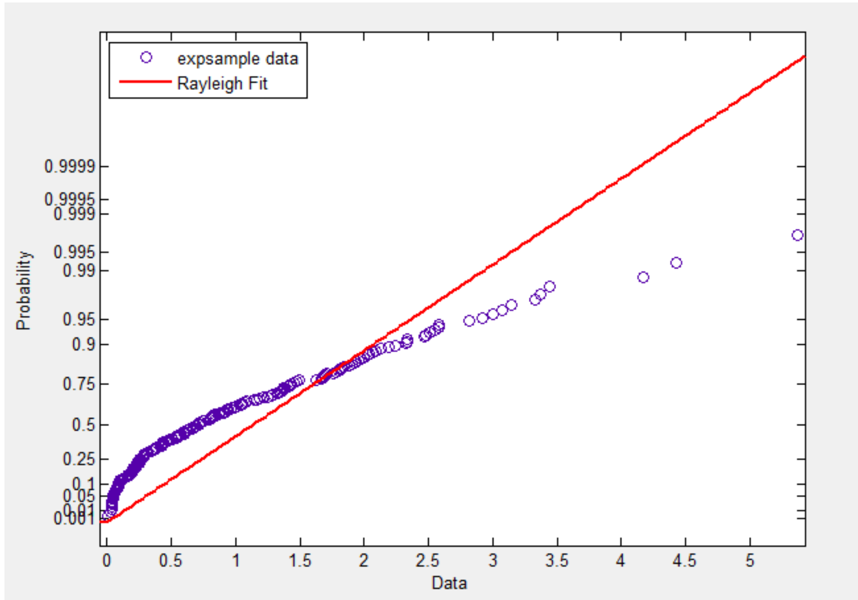

Figure 3.6 – Rayleigh probability plot of exponential distribution

3.3 Statistical Overlap Factor

Statistical overlap factor is defined by [23]

$$S_i = \frac{2\sigma_i}{(\omega_{i+1} - \omega_i)} \tag{3.7}$$

Or

$$S = \frac{2\sigma}{\mu} \tag{3.8}$$

σ is the standard deviation of a natural frequency from its mean

μ is the mean frequency spacing

The meaning of statistical overlap factor is if 'S' is small natural frequencies vary by small amount but if 'S' is large, it indicates natural frequencies move significantly. It was stated that system under rain-on-the-roof excitation wound show stationary in mean when statistical overlap factor is greater than 2 and 3 for steady mean behavior of system under point forcing[23].

4. Experimental Design and Setup

4.1 The plate

The studied plate is a steel circular plate. It is of 500 mm in diameter and 5 mm in thickness. To stimulate variation or uncertainty in material stiffness in the system, a number of aluminium bar are fixed on to the plate. As the statistical measure used need to be done across a set of similar structure but different variation, it would require to manufacture a great number of similar interested system. This is not effective in practical sense point of view. It, however, would be identical if only one perfect test system is used but a number of variations can be stimulated on this system. The plate is then required to be able to accommodate variation of location of the aluminium bars. The design, therefore, was based on changing of the aluminium bar's orientation. The fastening method employed was mechanical in which is screwing. The plate was be drilled with 1/8 inch drill (3.175 mm) which allow M3 screw to go through and tighten with the bars that are previously threaded at both ends. The dimensions of bars are 150 mm in length, 10 mm in width, there are 2 thicknesses which are 1 mm and 2.5 mm. The plate will accommodate maximum of 10 aluminium bars, each of the bars have 3 orientations as in figure 4.1, the straight lines represent possible set up. The holes that have been drilled are predetermined. The CAD drawing and real picture of the plate is in Figure 4.2.

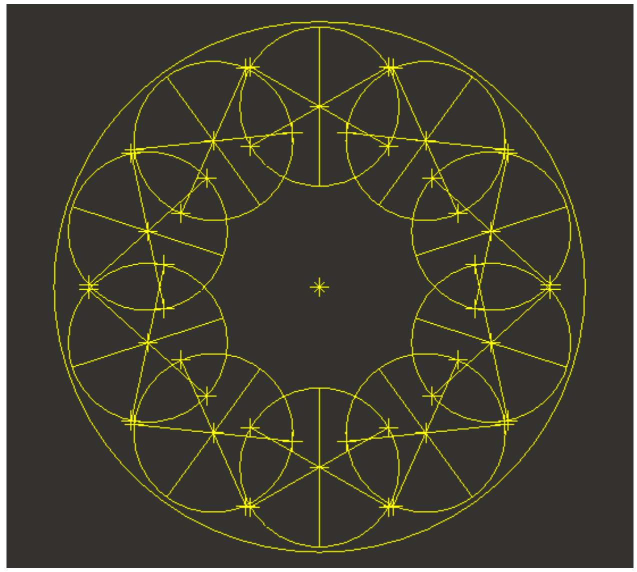

Figure 4.1 – Schematic diagram of circular plate

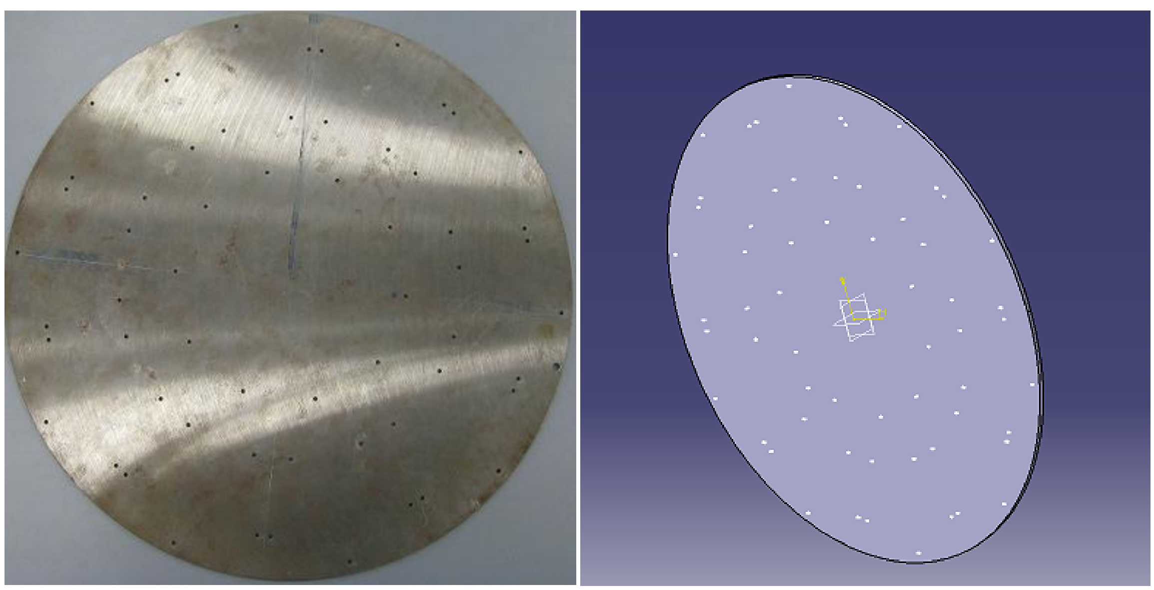

Figure 4.2 - Steel Plate (Left) and CAD drawing (Right)

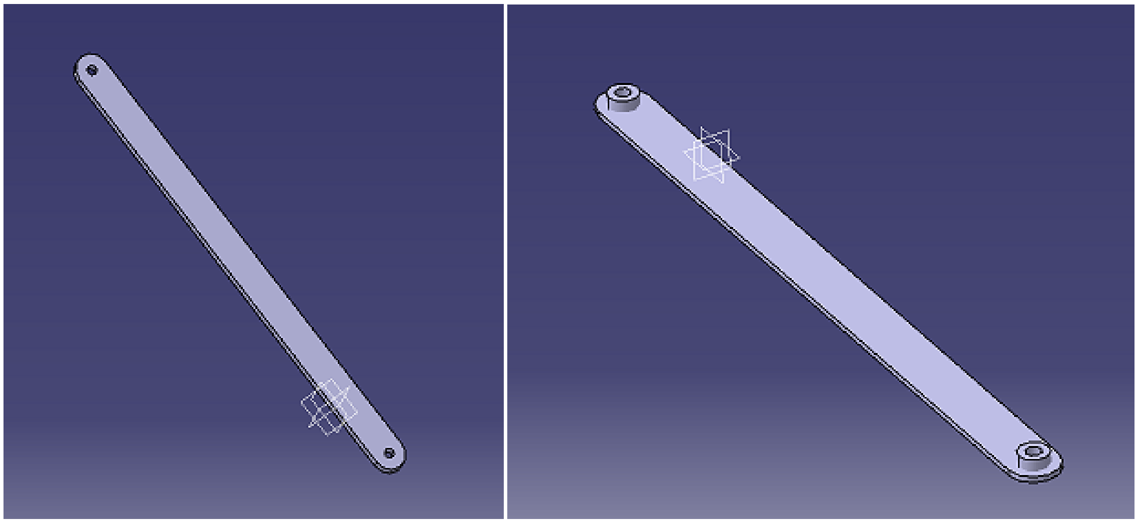

Figure 4.3 – Aluminium Bar of 2.5 mm (Left) and 1 mm (Right)

4.1.1 Aluminium bar

Aluminium was chosen in order to keep the mass as low as possible while providing a considerably stiffness. The density of aluminium is 2700 kg per m^3 where steel has density 7800 kg per m^3, when all 10 bars of length 150 mm, width 10 mm and thickness 2.5 mm are fixed on the plate the mass added is 0.10125 kg. The mass of the plate of diameter 500 mm and thickness of 5 mm is 7.658 kg. The mass of aluminium is $\frac{0.10125}{7.658} =$ 0.01322 or just 1.322 % of the plate. The mass of 1 mm thick bar is accounted for 0.0529 % of the mass of the plate. This is in order to keep the effect of variation in mass as low as possible to observe only stiffness permutation. This was ensured by the reviewed literature [9] showing that a total of 10 % mass variation with 10 points permutation did not have great effect on the system having low SOF and exponential distribution of natural frequency spacing. Effect of The aluminium bar will create local stiffness which will vary the natural frequencies of the plate. As the bar will be randomly placed on the plate, different orientation will differently affects each mode of vibration some at great degree, some at lesser degree. The local stiffness will not only change the natural frequencies but also the mode shape of the system as well. The bar will distort the mode where they are fixed, the vibration amplitude would be expected to be higher as stiffness is increased. The CAD drawing of 2 types of aluminium bars is in figure 4.3

4.2 experimental set up and techniques used

4.2.1 Supporting method

The boundary condition desired is free. The free condition means the test structure is completely isolated from ground and have rigid body mode at 0 frequency. In practical sense, it is not possible to achieve truly floating structure in space, it is needed to be support in some manner. Hanging structure from elastic band will in effect cause the rigid body behaviours to shift away from 0 frequency. If the elastic band's stiffness is low enough, and hence the frequency is much lower than flexible mode, the effect will often be negligible. Elastic cable was used in this experiment to hang the plate vertically from the ground. Before experiment the plate was given motion in vertical direction and perpendicular direction to the direction of the suspension to check if is frequency is low. The plate was vibrated at around 1 to 2 Hz, it was then concluded that the suspension was valid to perform experiment given adequate free condition. The setup is in figure 4.4.

Figure 4.4 – Suspended plate

4.2.2 Excitation

Impact excitation was chosen to perform experiment as it is a quick and require a few setup procedure. Impact hammer consists of hammer, a force transducer and hammer tip. The wave form generated by this type of excitation is transient. Since the force is impulse, the energy level transfer to the structure is determined by velocity and mass of hammer. This follows the theory of linear momentum. The measure force is the mass of the impactor behind the piezoelectric of disc of the force transducer times the acceleration. The true force, exciting the structure is the total mass of hammer times the acceleration during impact. The true force is the measured force times the ratio of total mass over the mass behind the transducer [24]. The duration and shape of the spectrum is determined by the mass and stiffness of both structure and hammer. The stiffness of the hammer tip determines the frequency range when hammer is used on relatively large test structure. The harder the tip is, the shorter the pulse which means higher frequency range covered by the impact. The tip, however, should be chosen as soft as possible for the interested frequency range to prevent the leakage of energy to frequency which is outside the range of concern. The useful frequency range is from 0 Hz to a frequency point where spectrum magnitude has decayed by 10 – 20 dB.

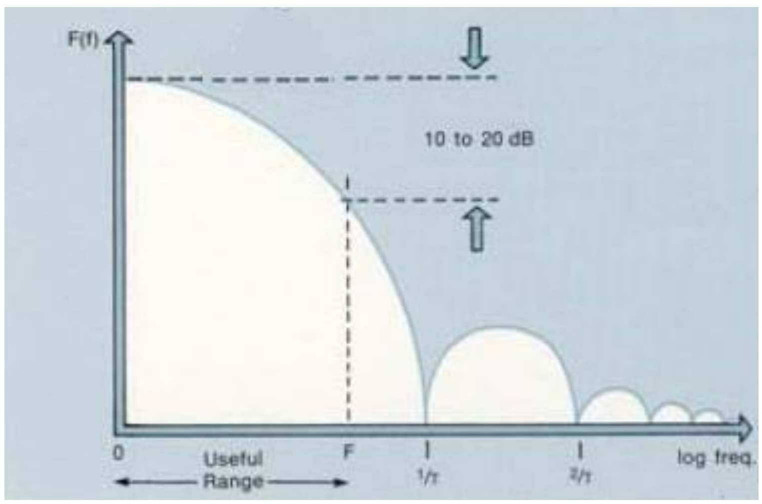

Figure 4.5 – Hammer Force Spectrum[24]

The experiment was performed at the range of up to 6000Hz, the frequency range is considered high when impact hammer is used. The tip was chosen by checking the hammer spectrum whether it provided enough energy across the range. Steel tip was chosen because it was decayed by about 18 dB across the range

Hammer, although, regarded as the quickest and convenience excitation choice, it is difficult to obtain a consistent result, since it is difficult to control the velocity of the hammer. The force spectrum cannot be band-limited at lower frequencies which mean that the technique is not suitable for zoom analysis. Another 2 problems that might be raised during the experiment and need to be taken into account are noise and leakage. Noise can be experienced in both input force and response due to long period of record. The second problem, leakage, can be present in response signal as a result of a short record time.

4.2.2.1 Double hit

Double hit is occur when the struck structure bounced back to the impacting hammer, there will more chance of double hit with increase hardness of the hammer tip especially steel tip. Force signal will reveal 2 or more sharp peak and the spectrum will not be smooth, if this occurs the record will be disregard. It cannot be compensate by using transient window or any other windows.

4.2.3 Windowing

Since the force signal is usually short when compared to the duration of the record time. The force signal beside the period of impact is noise and can be eliminated without affecting the pulse itself using window technique. The window to use is transient window, this takes out any signal outside the window but it is that short oscillation after pulse is actually part of the pulse and should not be disregarded.

The response signal might, as well, suffer error. There are 2 situations where the error may arise. The first scenario is when the structure is lightly damped which the record time is shorter than decaying time. The second case rose if the test structure is heavily damped in which its response decay really fast and end much faster than the record time. The first case will introduce leakage error whereas the second case will have poor signal to noise ratio because the measurement is suffered from noise.

This is when exponential window is employed; it can handle well both situations. The window function is given by

$$w(t) = e^{\frac{-t}{\tau}}$$

Where

τ is time constant

The window will minimise the leakage error in the first case by forcing the response to decay completely before the end of record time. This, however, bring in the extra damping to the system resulting in broader resonance frequency. It can be corrected on the post processing stage.

It eliminates the remaining noise in the measurement in the case where response dies out before the end of record time. The selection of the time constant, (the time required for the amplitude to be reduced by a factor of 1/e), is about one-fourth the time record length.

4.2.4 Striking location

The striking location was chosen at where there is no aluminium bar fixed. As the experiment is only interested on the location of natural frequencies, the striking location could be change for every set of configuration. The coherence was check if the striking location was on a nodal line. At each set of configuration several place was tested to find optimum point where it revealed the most modes.

4.2.5 Location of accelerometer

The location of transducer can be any point of interest provided that it is not on or close to a node or more of the structure's modes. It will be difficult to make an effective measurement. Similar approach to striking location was used, if poor coherence was experienced location of accelerometer was changed but kept constant for each configuration to find the optimum location to record point.

4.2.6 Coherence

Coherence function is given by [2]

$$\gamma_{FX}^2(\omega) = \frac{|S_{FX}(\omega)|}{S_{FF}(\omega) S_{XX}(\omega)}$$

$S_{XX}(\omega)$ is output spectrum

$S_{FF}(\omega)$ is input spectrum

$S_{XF}(\omega)$ is cross spectrum

$\gamma_{FX}{}^{2}(\omega)$ is between 0 to 1. Coherence is a measure of linear relationship between input and output for each frequency. It will show 1 for no noise measurement while 0 indicates pure noise measurement. The coherence that is less than perfect 1 indicates poor signal to noise ratio, number of measurement errors, structure's nonlinear behaviour, inadequate frequency resolution or a combination of more than 1 error.

The use of coherence function on impact testing is limited due to deterministic nature of the signal coherence function cannot show either leakage or nonlinear behaviour. The source of less than 1 in coherence function are the signal to noise ratio is poor at anti resonance, not striking the test structure perpendicularly with surface and impact point is at or near nodal point which often result in very low coherence . Figure 4.6 shows a sample of good measurement where coherence reveals 1 everywhere except around anti-resonance.

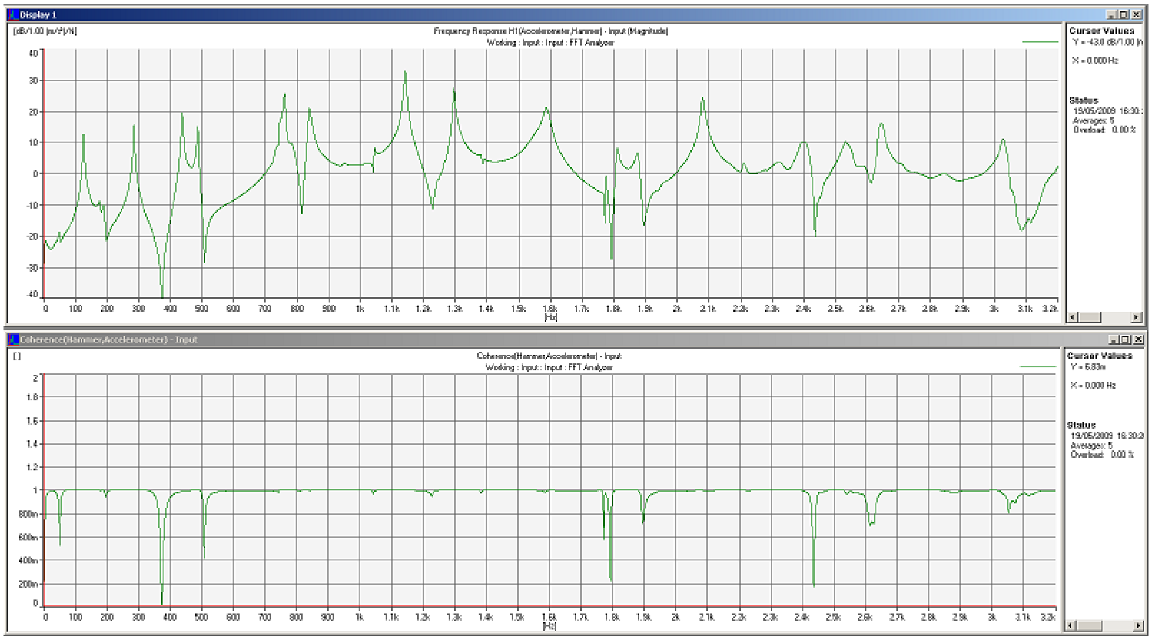

Figure 4.6 – Sample Coherence

4.2.7 Measurement analysing

As this experiment is only interested only on the location of the natural frequency, no other post-processing is required. Figure 4.7 shows a sample of frequency response which each peak represent natural frequency which can be read of the display using program cursor.

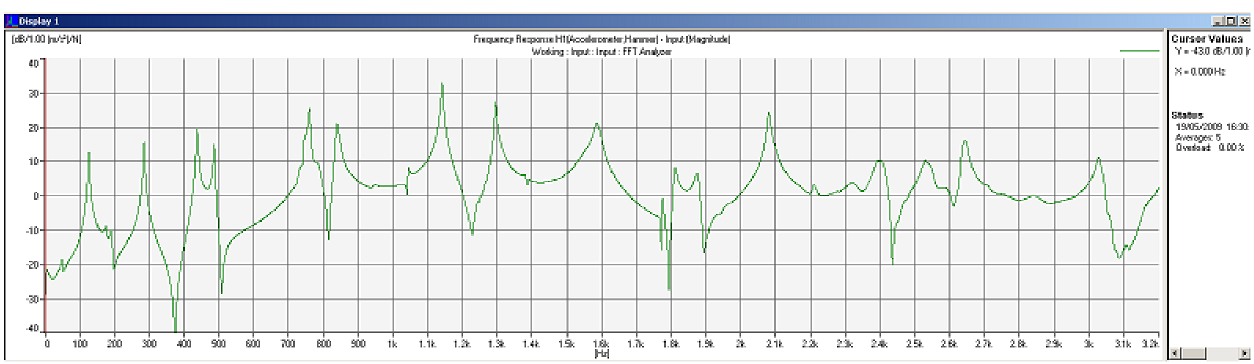

Figure 4.7 – Sample of frequency response

It might be, however, possible that some peak may not obvious or verification was needed. This is when Nyquist plot technique was employed. It is the plot of real part against imaginary part of frequency response function. If it plotted range just cover the resonance region, the plot will be circular as in the sample plot of obvious peak at 125 Hz from figure 4.7 is illustrated in figure 4.8. Only frequency points closest to resonance are identifiable because those away from resonance are very close together [25]. Any uncertain peak with non-circular Nyquist plot was disregarded from analysis.

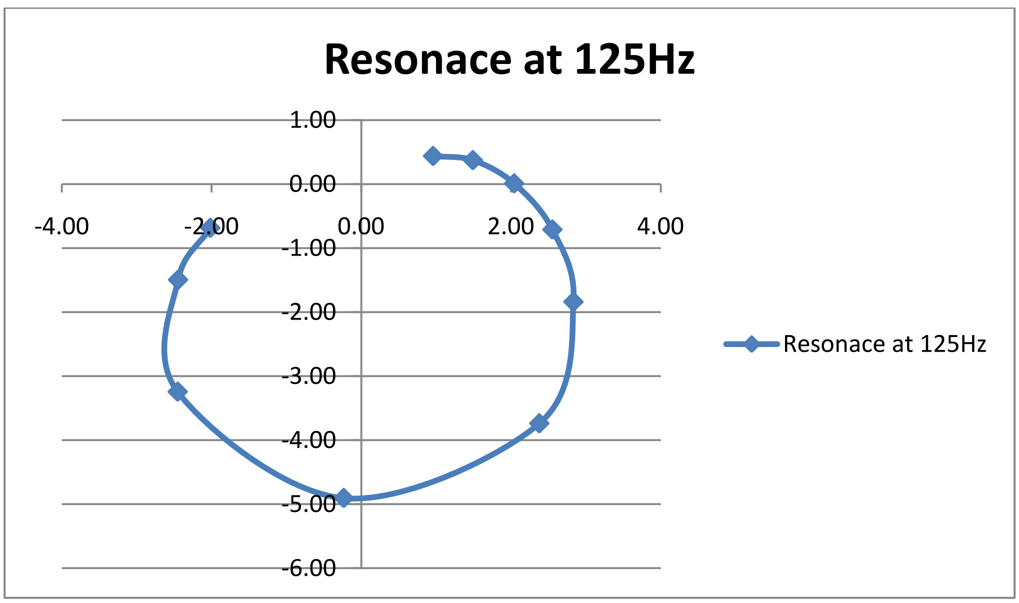

Figure 4.8 – Nyquist plot

4.2.8 Summary of equipments

Equipment	Name of equipment
Personal Computer installed with Pulse software	HP Laptop
Data logger	Bruel & Kjær Pulse FrontEnd Type 3560C
Charge Amplifier	Bruel & Kjær Type 2635
Piezoelectric Accelerometer	Bruel & Kjær Type 4393
Impact Hammer	Bruel & Kjær Type 8202
Force Transducer on hammer	Bruel & Kjær Type 8200
Elastic Cable	

Table 4.1 - Summary of equipment

4.2.9 Equipment setup

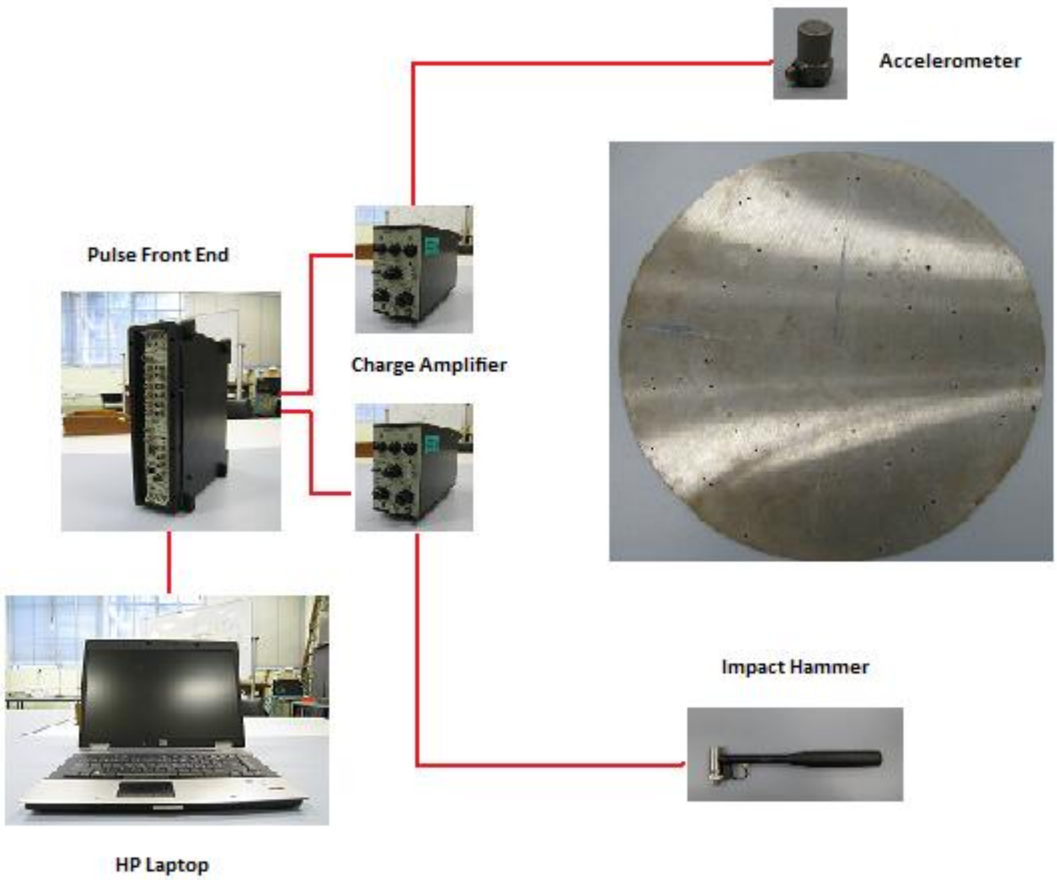

Figure 4.9 - Equipment setup

4.2.10. Randomisation the location of aluminium bars

The orientation of each of the bar 10 bars were random using MATLAB. Each orientation in each circles representing the possible orientation were assigned with a number 1 to 3 as in the sample circle in figure 4.10. A set of number will be randomly generated by MATLAB function called 'randint' where it generates a random integer with specified row, column and integer range. The sample full command is the following

ans=randint(1,10,[1,3]);

The command will generate 1x10 integer matrix with random integer between 1 to 3. The generated matrix was to position the aluminium bar. The step was repeated if more configuration is required. The sample output is below.

ans = 3 3 2 3 1 2 3 3 3 2

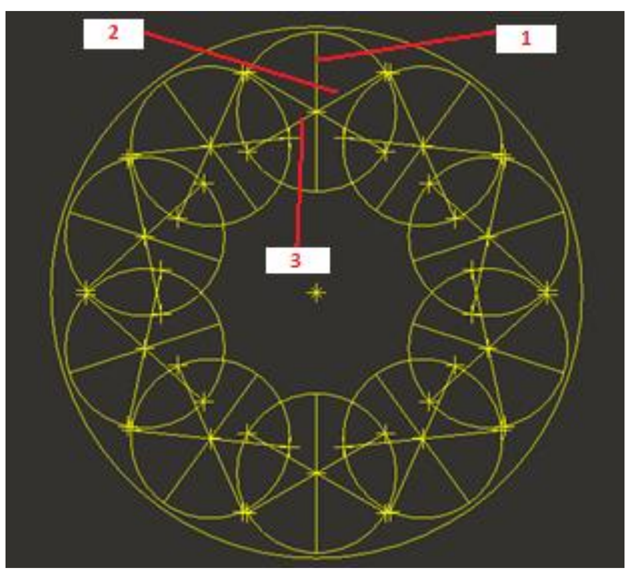

Figure 4.10 – number assignment

5. Result and Discussion

5.1 Experimental result

25 samples were measured to use in analysis phase.

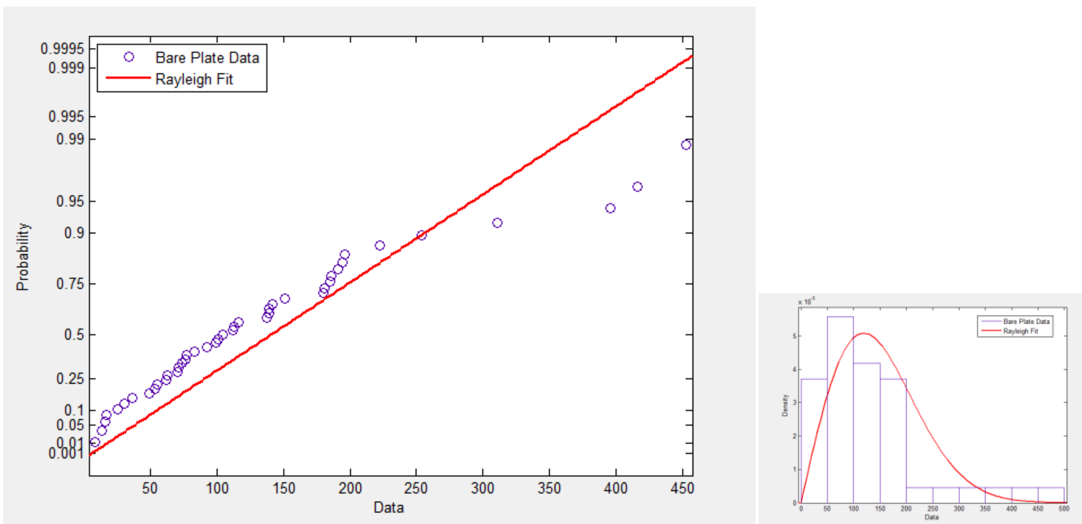

Figure 5.1 – Bare plate probability plot and histogram

The negative mass was found to have great influence on the system when compared to perfect solid circular plate. The plate has holes that were made to fix aluminium bars. Each hole has dimension as described in previous section chapter 4, a diameter of 3.175 (1/8 inches) with drilled through the plate of 5 mm thick. The steel plate has diameter of 500 mm therefore each hole is effectively is a 3.175/500 fraction or 0.635 percent negative mass of the total mass of the plate. The histogram and Rayleigh probability plot is in figure 5.1 showing a close match to Rayleigh.

The plate was designed to have 60 holes. It is however, when perform the experiment there were 10 bars fixed on the plate, the hole were filled with screw, therefore only 40 holes were left on the plate but the following result showed that they are still strong effect on most of response in which there were little change on the spacing distribution.

The frequency range in figure 5.2 to 5.4 is 200Hz to 6000Hz, 10 of 2.5 mm thick bars were used

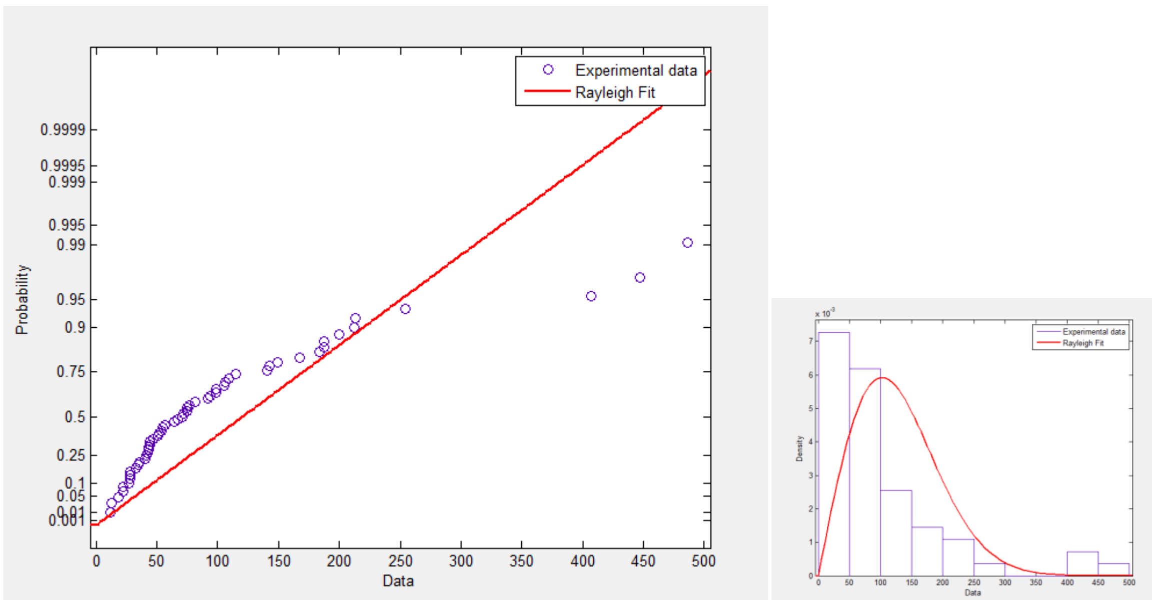

Figure 5.2 - Sample of experimental result probability plot and histogram that tend toward exponential distribution

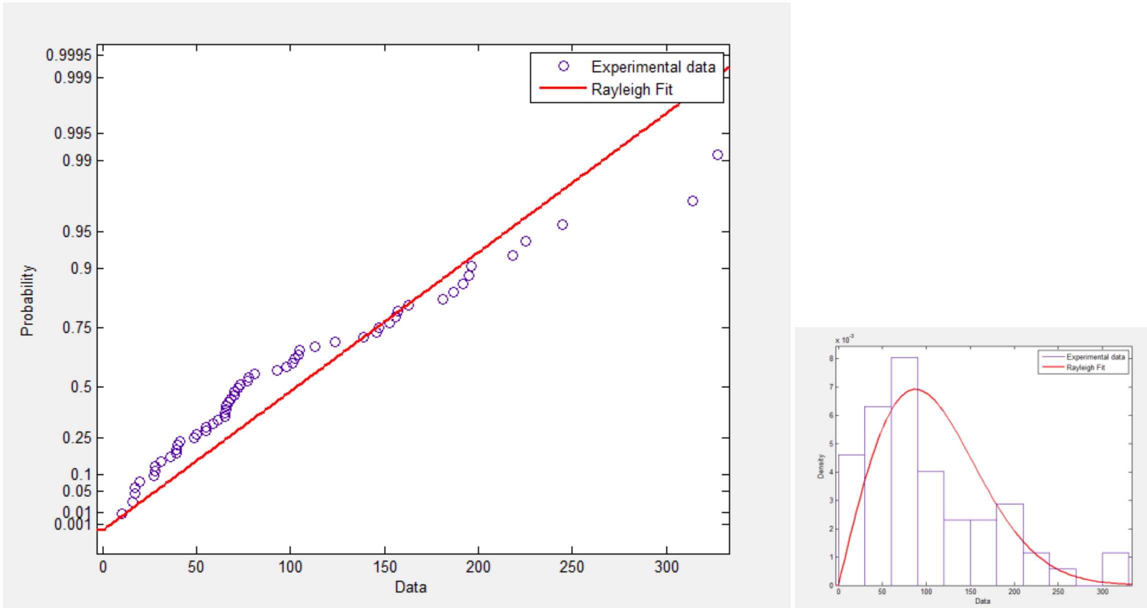

Figure 5.3 - Sample of experimental result probability plot and histogram that tend toward Rayleigh distribution

Since the plate showed the Rayleigh distribution even though the aluminium bars were not attached, the response will be use as a benchmark to observe and effect of mass stiffness permutation, figure 5.1 showed the spacing distribution of the bare plate. 80% of results showed a Rayleigh distribution which in this case means that the aluminium bar was with no significant different to the match to Rayleigh. This effect can be concluded as neglectable or little. It, however, the fact that the 20% of the result showed the shift back toward exponential. This would be a result from counter effect of the aluminium bar as well as location and orientation of the bar to counter the effect of negative mass.

This similar effect has been previously observed by Fox [26] which used mass to attach to specific location to change specific natural frequency so called mode trimming where he trimmed the natural frequencies of an imperfect ring to eliminate certain of the frequency splits present.

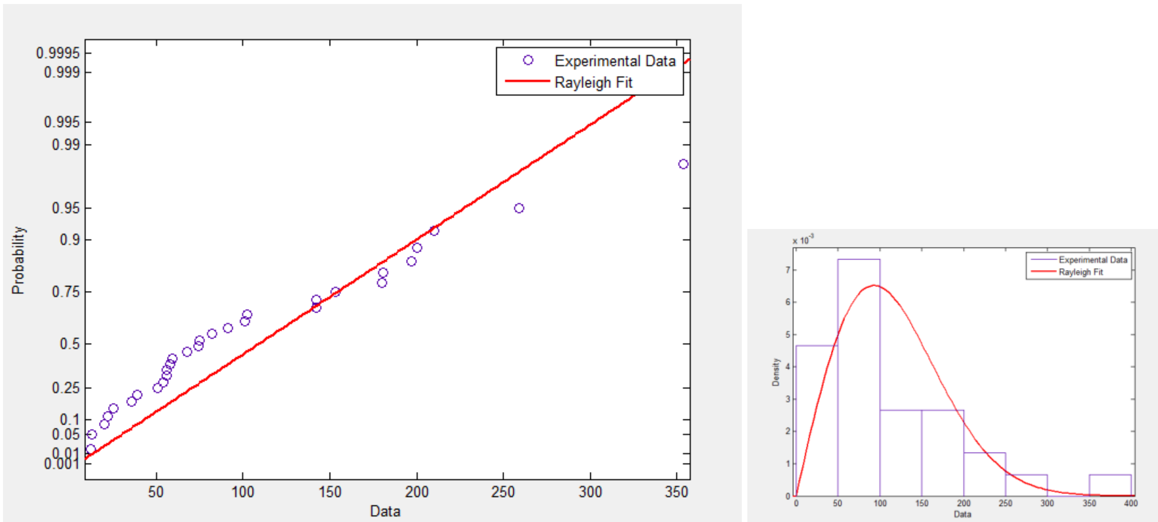

Figure 5.4 - sample of experimental result probability plot and histogram that tend toward Rayleigh distribution between 200Hz to 3000Hz

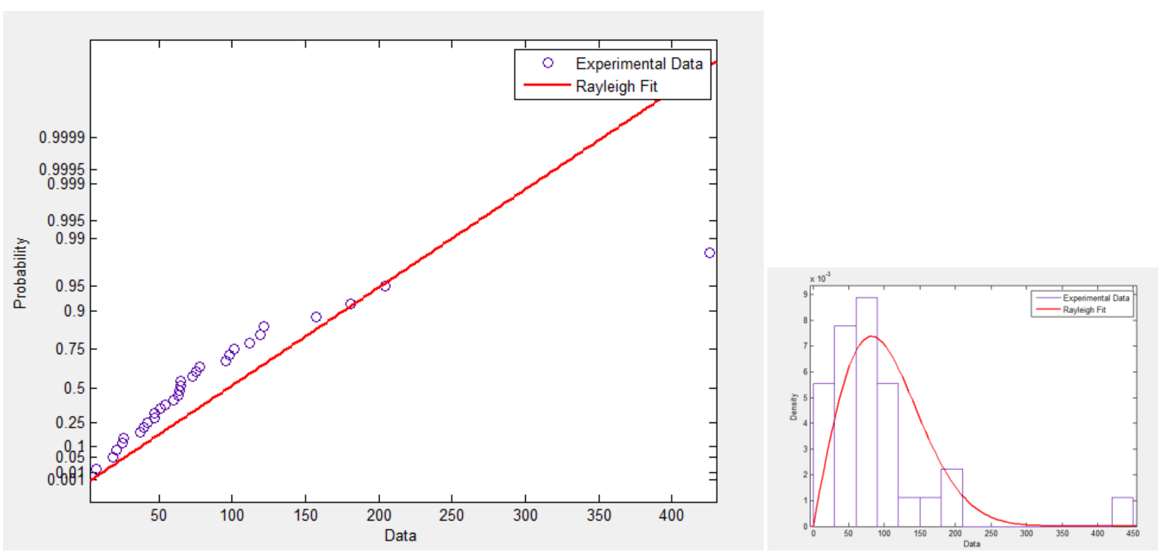

Figure 5.5 - Sample of experimental result probability plot and histogram that tend toward Rayleigh distribution between 3000Hz to 6000Hz

The most results are similar to figure 5.4 and figure 5.5 which of the result in the range of 200Hz to 3000Hz and 3000Hz to 6000Hz respectively. There were no significant different in the 2 plotting range where the effect was concluded to be neglectable or little even at higher frequency.

5.2 Simulation Result

As the system which has been built showed that it was really sensitive to negative mass variation. Simulation was employed to study the perfect circular disc behaviour subjected to mass stiffness uncertainty. ANSYS was used to model steel disc from the one that used in experimental study but holes were neglect to create a perfect symmetric vibration. The simulation revealed vibration which occurred in pair as expected. The sample of natural frequency of the plate is in table 5.1. The model was then modified to contain aluminium bar which bonded to the steel plate model. The models which had different number of bar was also studied. This was to observe any change when number of variation was increased, there were 10, 30 and 50 bar models created, 10 different configuration were made for each type. The volume of material added was constant, the higher number of bar, the shorter the length. It thickness and width were kept constant. The sample of models of 10, 30 and 50 bars is in figure 5.6, figure 5.7 and figure 5.8 respectively.

Mode Number	Natural Frequency
7	104.08
8	104.10
9	175.05
10	241.29
11	241.30
12	397.54
13	397.67
14	423.07
15	423.08
16	648.23
17	648.24
18	683.64
19	683.65

Table 5.1 – Sample of natural frequency pairs

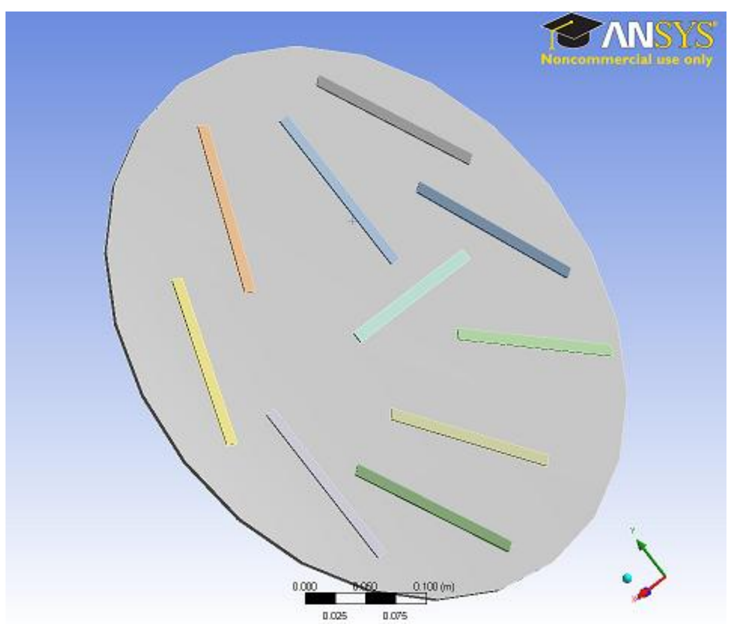

Figure 5.6 – 10 bars Plate model

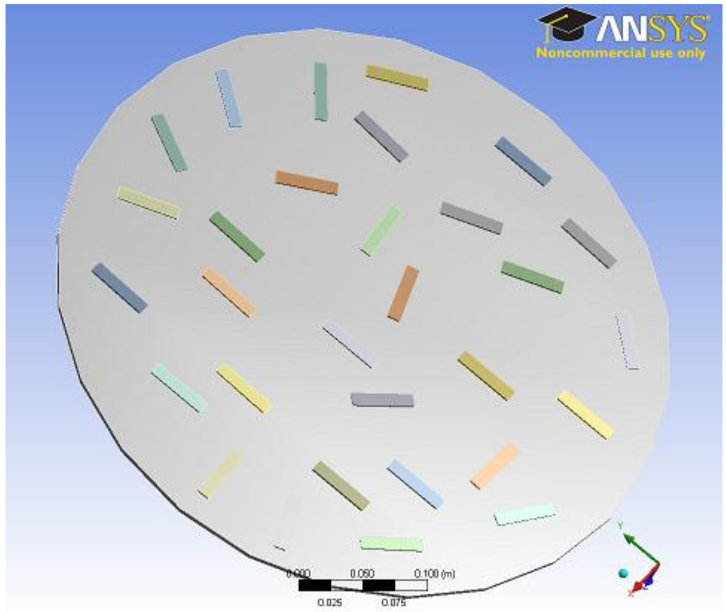

Figure 5.7 - 30 bars Plate model

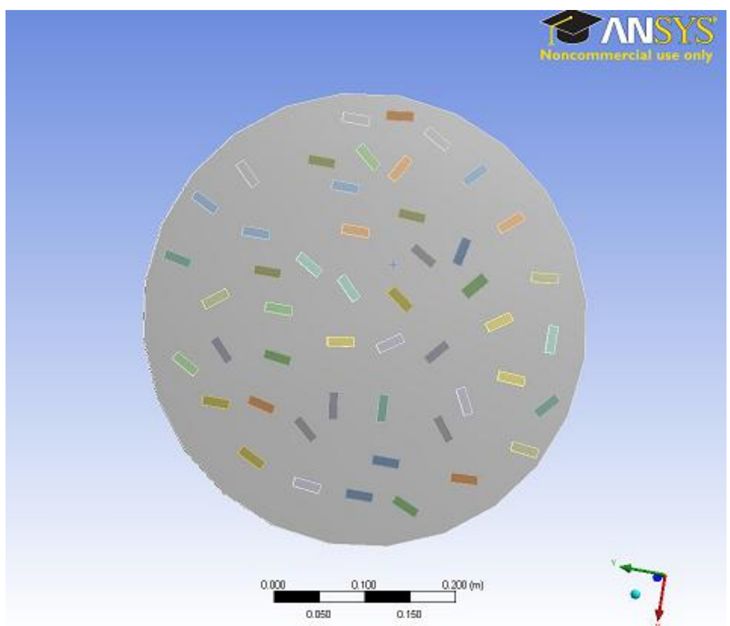

Figure 5.8 – 50 bars Plate model

The comparisons were made on natural frequency spacing distribution of a steel circular plate subjected to 10, 30 and 50 material stiffness permutation. Material stiffener used was a thin aluminium bar of Young's modulus = 70 GPa which has the same dimension as the one that used in the practical experiment. The total volume material added was constant. It was first to perform the check if model's natural frequencies varied from the one of the perfect plate, the result is shown in table 5.2. The sample of modified plate was a member of the 10 bars model. It can be seen that the natural pairs were separated. No trend on splitting was observed. Most of the splitting was less than 5 Hz apart even at higher frequency (up to 6000Hz).

The rest of analysis was in the range from 200 Hz to 12000 Hz. Each sample from the simulation result is shown in figure 5.9 to 5.14 which are separated in 2 analysis range 200Hz to 6000Hz and 6000Hz to 12000Hz respectively to identify any change as frequency increased. The red line in probability plot is the fit for perfect Rayleigh distribution where the red line in histogram shows a Rayleigh distribution calculated using the samples mean.

Mode number	Bare plate	Modified plate
7	104.08	107.02
8	104.10	107.80
9	175.05	179.47
10	241.29	249.20
11	241.30	250.27
12	397.54	406.95
13	397.67	408.51
14	423.07	437.70
15	423.08	439.38
16	648.23	670.82
17	648.24	672.10
18	683.64	699.41
19	683.65	702.66
20	746.25	763.99
21	915.80	947.82
22	915.81	948.43
23	1025.80	1051.40
24	1025.90	1054.60
25	1159.30	1181.30
26	1160.00	1189.70
27	1225.00	1264.00
28	1225.00	1269.30
29	1420.60	1458.10
30	1420.60	1460.10
31	1575.10	1623.10
32	1575.10	1629.20
33	1632.80	1671.50
34	1633.00	1673.40
35	1699.60	1743.20
36	1865.50	1914.80
37	1865.50	1916.80
38	1965.60	2022.40
39	1965.60	2029.80
40	2161.40	2205.20
41	2161.90	2218.90
42	2298.90	2352.40
43	2302.00	2358.30

Table 5.2 – Comparison of natural frequencies

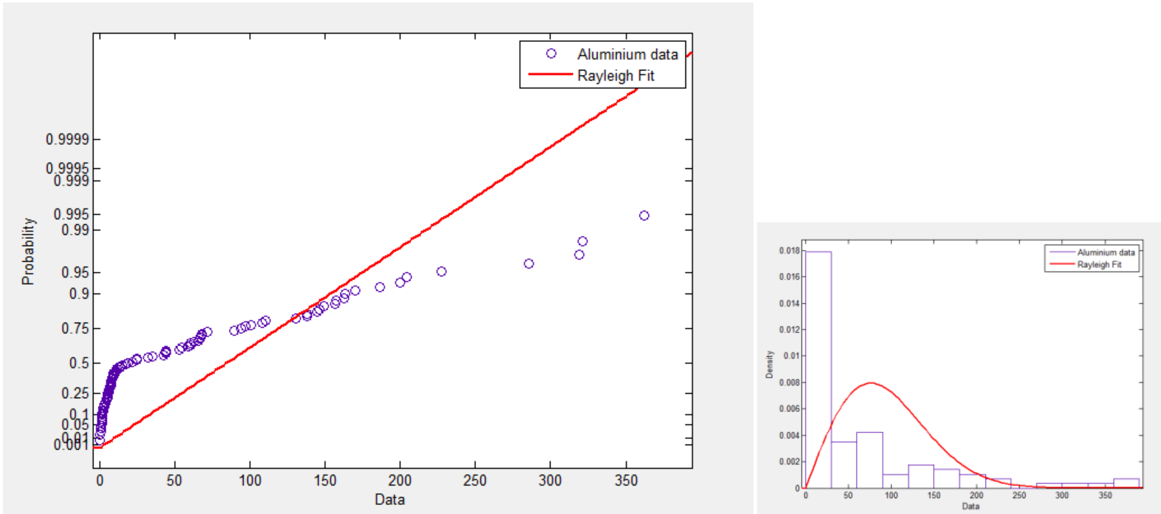

Figure 5.9 - Sample of 10 pieces model simulation result probability plot and histogram between 200Hz to 6000Hz

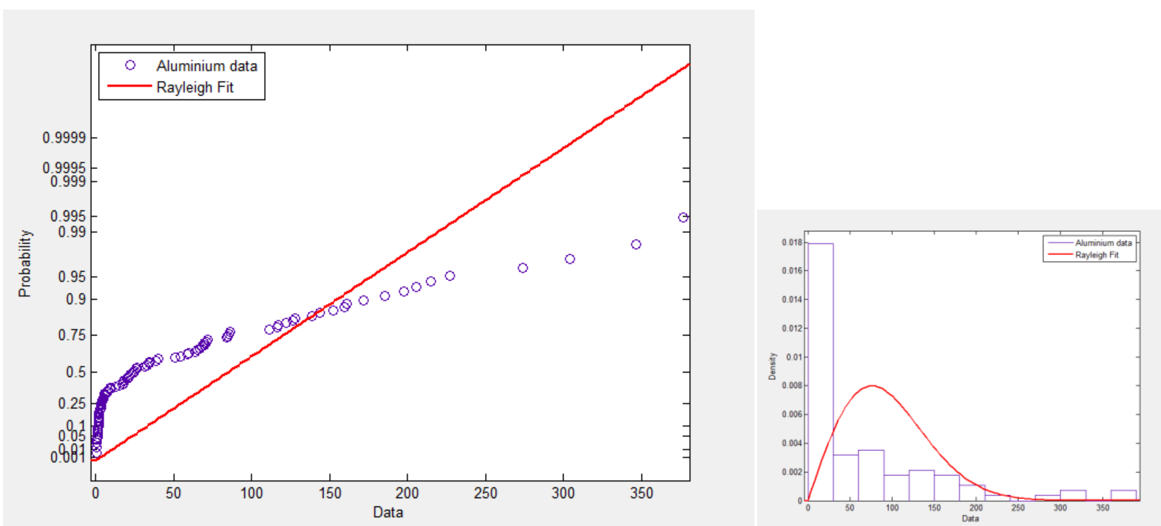

Figure 5.10 - Sample of 30 pieces model simulation result probability plot and histogram between 200Hz to 6000Hz

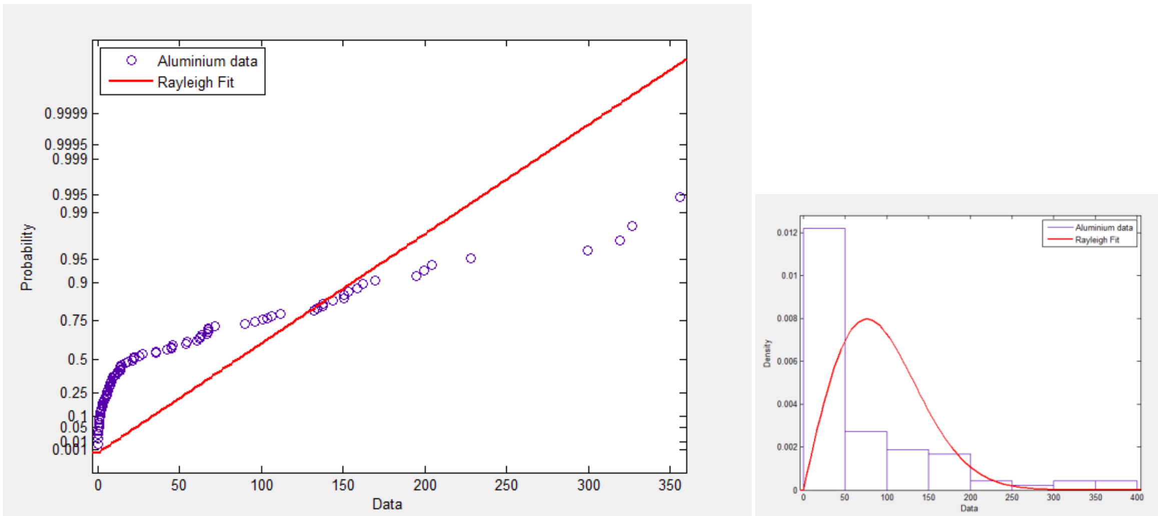

Figure 5.11 - Sample of 50 pieces model simulation result probability plot and histogram between 200Hz to 6000Hz

The result showed no significant difference among the sample. They showed a strong exponential distribution. The comparison of bare plate and permutated plates showed no different. This means that the aluminium bar had little or no effect on the system. This confirmed the validity of experimental result and that in overall the aluminium bar has too small effect on steel plate to make the response random enough to generate Rayleigh distribution. The result also revealed that mass of aluminium bar did not or rarely contribute to any effect on the result in experiment. The splitting of natural frequency pairs were also low even increasing the number of bar.

The frequency range in figures below is between 6000Hz to 12000Hz, which were from the same sample simulation result but the frequency range is from 6000Hz to 12000Hz

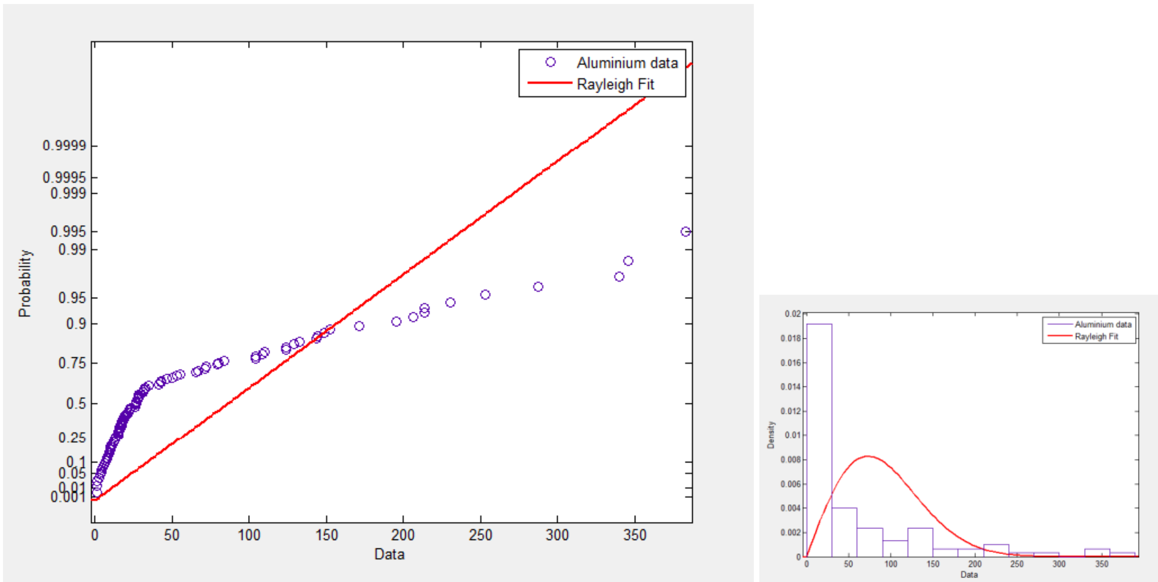

Figure 5.12 - Sample of 10 pieces model simulation result probability plot and histogram between 3000Hz to 6000Hz

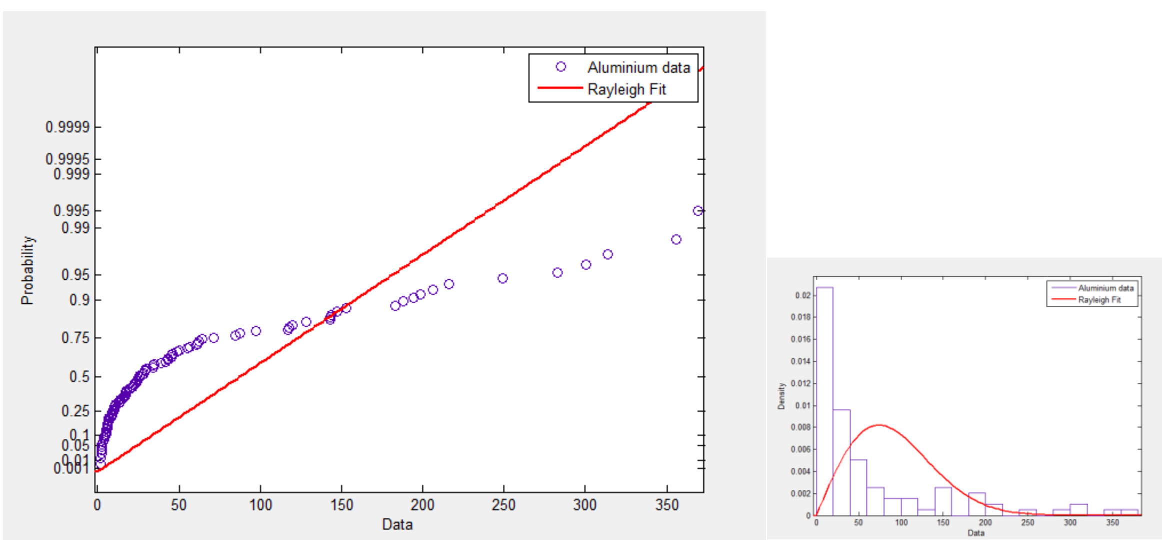

Figure 5.13 - Sample of 30 pieces model simulation result probability plot and histogram between 3000Hz to 6000Hz

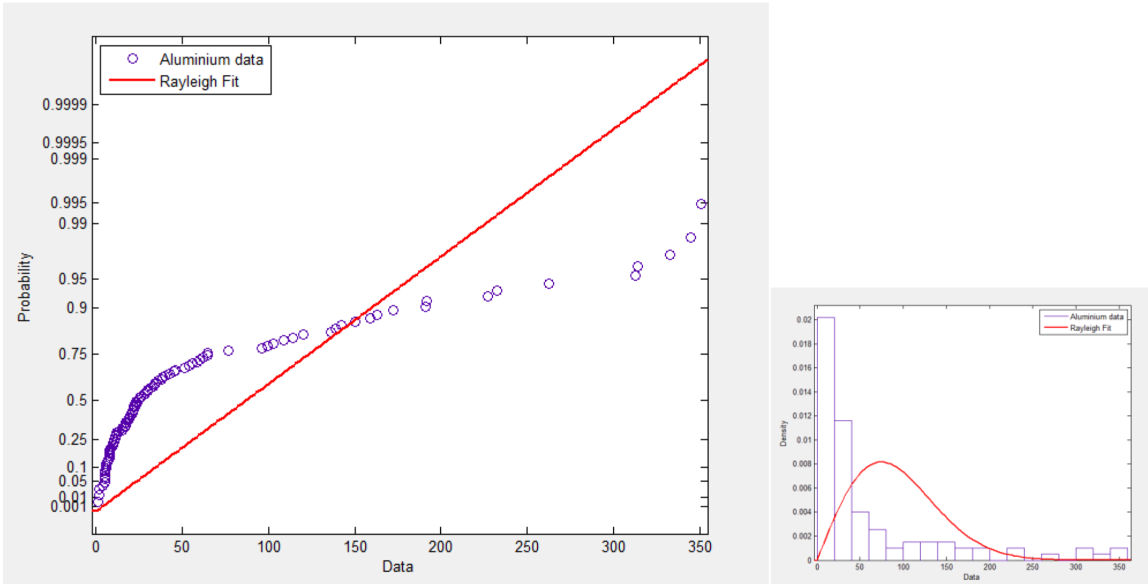

Figure 5.14 - Sample of 50 pieces model simulation result probability plot and histogram between 3000Hz to 6000Hz

There was still no significant change at higher frequency range. The distribution remain strong exponential. It was correspond to the experimental result where the 80 % of systems ensemble member did not or little change the system natural frequency spacing distribution from the original system.

The following section the simulation was used to find at what material stiffness, the system would response in a shift in natural frequency spacing to Rayleigh distribution. A range of stiffness has been test and at Young' modulus of 800 GPa, the splitting distribution started to depart from exponential distribution. It is noted here that the rest of material properties are of the aluminium which include Poison ration and density. This is to keep other variable constant to observe what the effects of variations in material stiffness are. Although in reality is merely impossible to have a material stiffness variation of 800 GPa which is almost of diamond stiffness,

Young's modulus of aluminium is edited to 800 GPa.

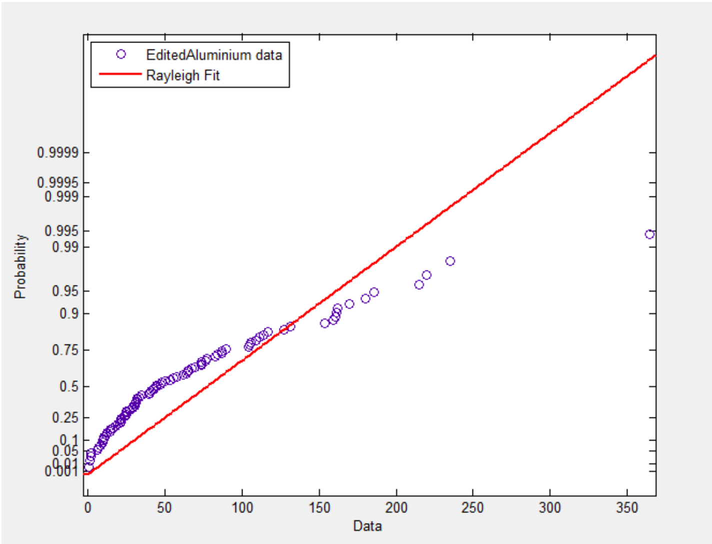

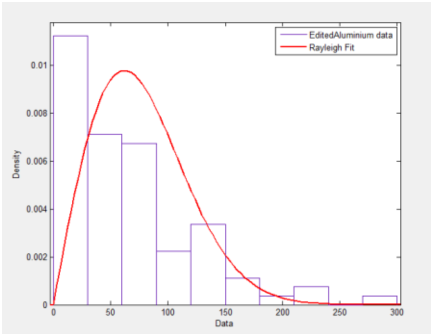

Figure 5.15 - Sample of 10 pieces model simulation result which stiffness is edited to 800GPa showing probability plot and histogram between 200Hz to 6000Hz

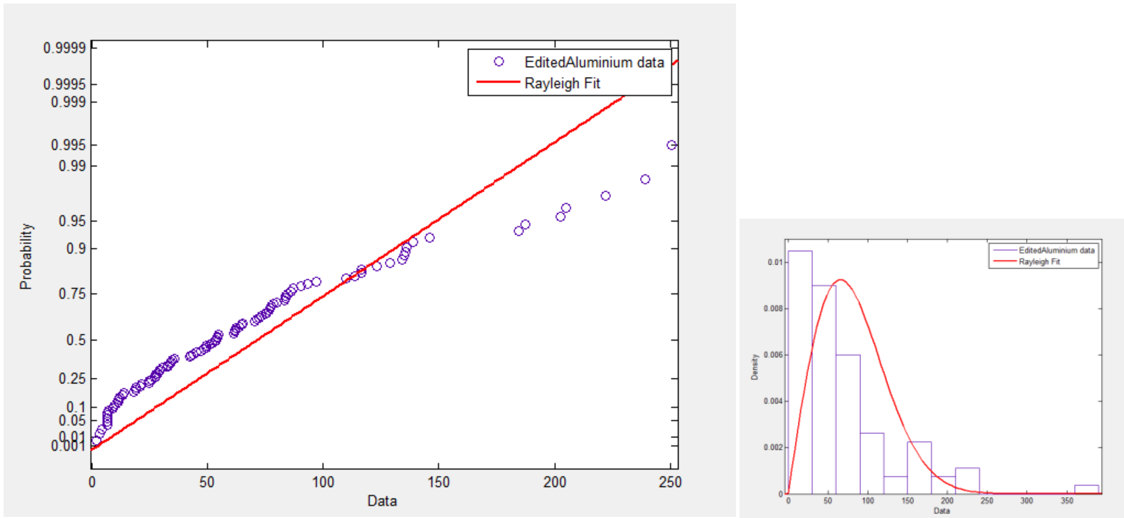

Figure 5.16 - Sample of 30 pieces model simulation result which stiffness is edited to 800GPa showing probability plot and histogram between 200Hz to 6000Hz

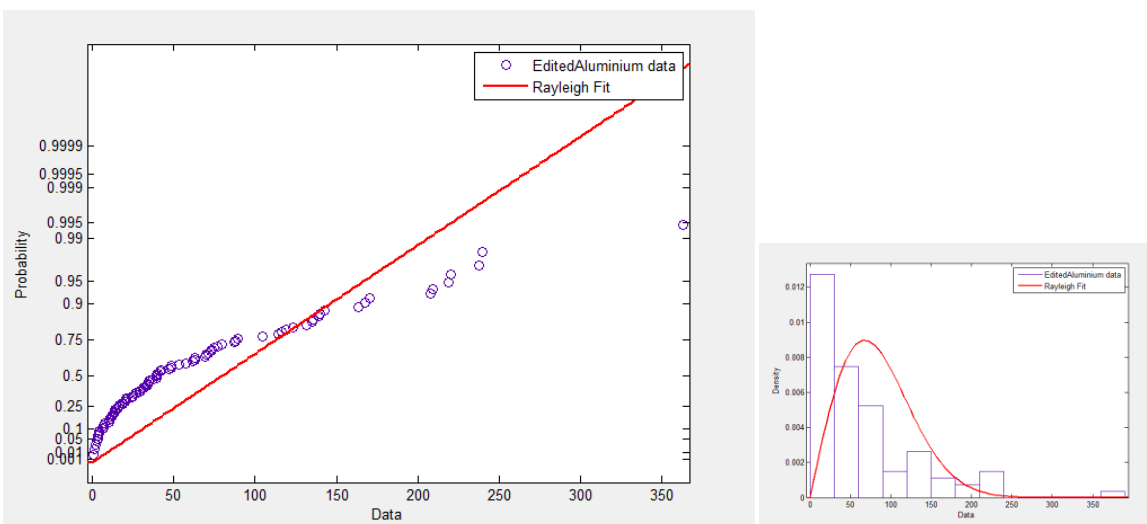

Figure 5.17 - Sample of 50 pieces model simulation result which stiffness is edited to 800GPa showing probability plot and histogram between 200Hz to 6000Hz

The sample histogram showed that at 800 Gpa , the closest match was when 30 pieces of aluminium bars were added. When 50 bars were used, the result shifted back towards exponential distribution. As the number of bar increased, keeping the total material added, the bar would be too small to interfere each mode which otherwise would vary natural frequency to be random enough to generate Rayleigh distribution. The higher number of bar would be expected to give a closer match to exponential distribution. The results were more clear and pointing to the same conclusion when the frequency range is between 6000Hz to 12000Hz which shown in figure 5.18 to figure 5.20.

Figure 5.18 and figure 5.20 shown below are the sample natural frequency spacing of range between 6000Hz to 12000Hz using the same sample as above 200Hz to 6000Hz

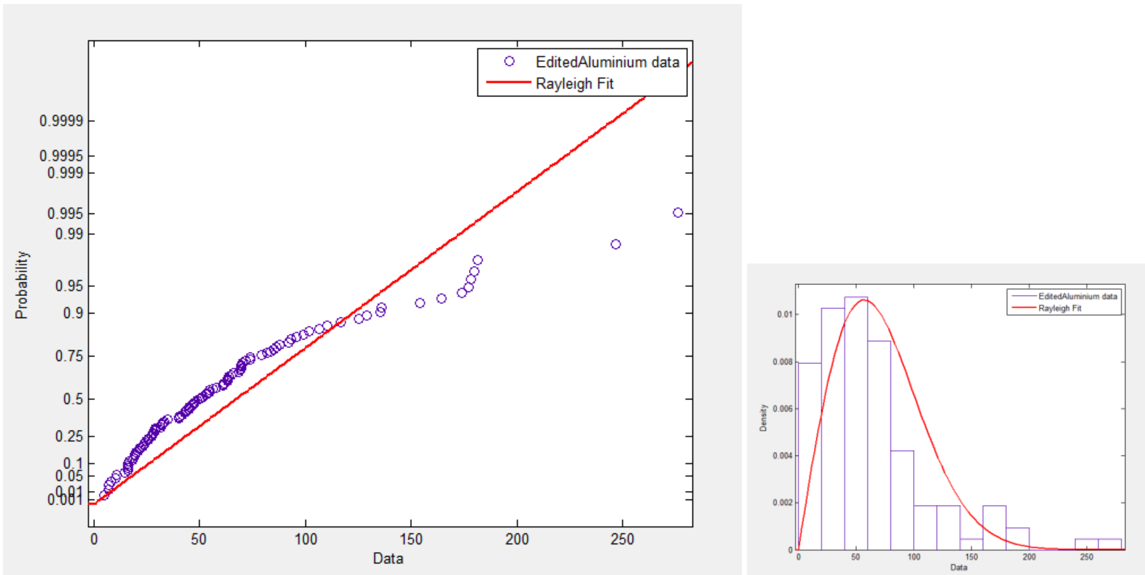

Figure 5.18 - Sample of 10 pieces model simulation result which stiffness is edited to 800GPa showing probability plot and histogram between 200Hz to 6000Hz

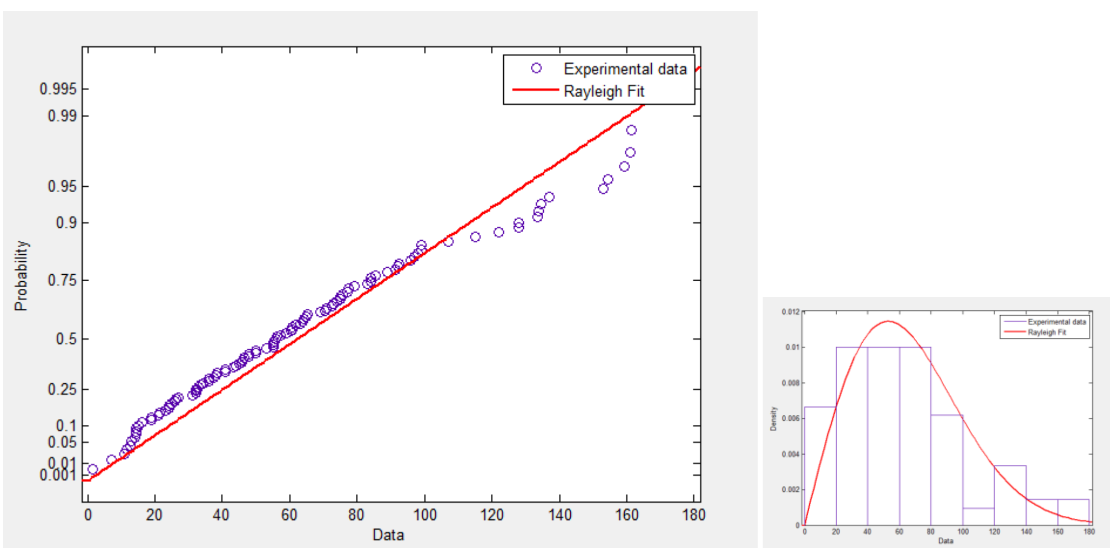

Figure 5.19 - Sample of 30 pieces model simulation result which stiffness is edited to 800GPa showing probability plot and histogram between 200Hz to 6000Hz

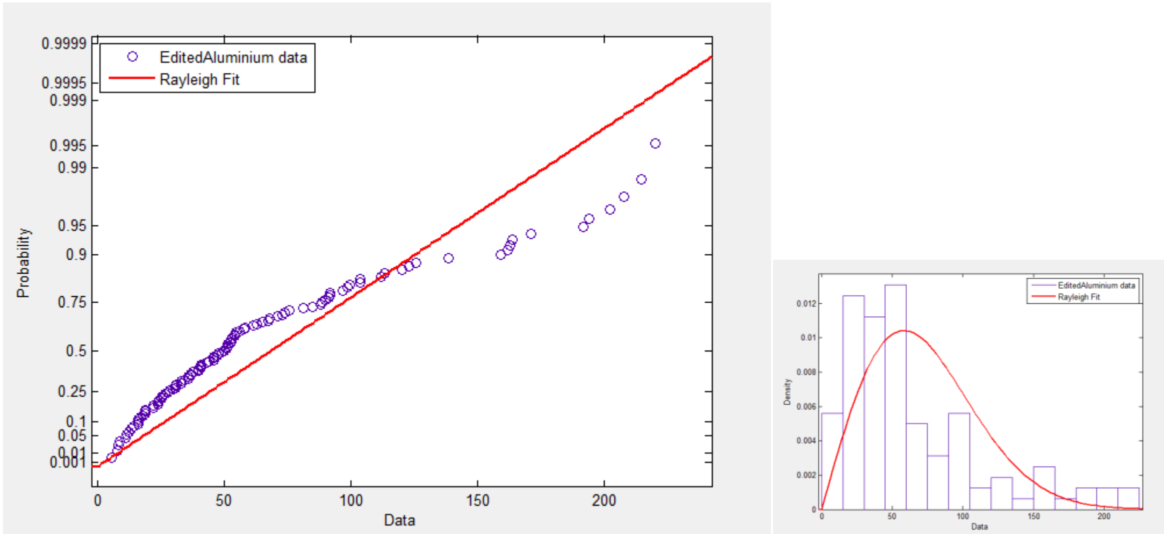

Figure 5.20 - Sample of 50 pieces model simulation result which stiffness is edited to 800GPa showing probability plot and histogram between 200Hz to 6000Hz

It has been observed that the higher the frequency the closer match to Rayleigh distribution. The effect of material stiffness randomness was increasing as the frequency got higher. Again, the result coincided with the lower frequency range where 30 bars system was found to be the closest match.

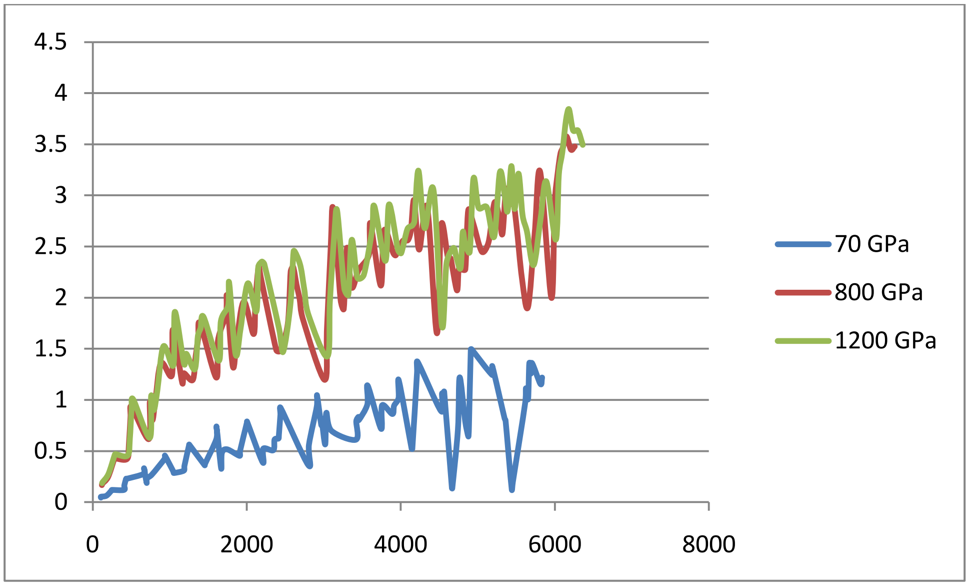

Figure 5.21 – Statistical Overlap Factor of simulation results of 10 bars model

Figure 5.21 shows statistical overlap factor of the system with 10 bars added. Samples of natural frequency spacing's histogram as well as the rest of result showed a mismatch to Rayleigh when stiffness is 70 GPa. The SOF for the system with the bars stiffness is 70 GPa is quite low therefore matched with the plot of natural frequency spacing where all samples show a strong exponential distribution and the splitting of natural frequency pairs were still close apart.

When the stiffness was edited to 800 GPA, the SOF increased to a highest of value of 3.7 but the sample of natural frequency spacing histogram the previous section still did not show a perfect match to Rayleigh because the SOF still fluctuate a lot between high and low value. This indicate that only few certain natural frequencies were very vary but not enough to make the overall system response random.

6. Conclusion

The designed system was proved to be a not effective studied tool, it however still gave a considerably amount of result which were useful information. From both simulation and experimental results, it can be concluded that the effect of mass permutation were very low whereas negative mass has strong effect as in the same situation as the positive mass variation case.

The mass variation effect on the natural frequency spacing has been commented in many articles that it was the source of randomness in response over spring stiffness and damping stiffness. The effect of negative mass is strong even in the bare plate where the holes on the plate are symmetric, the natural frequency spacing resulting from the splitting of natural frequency pairs showed a Rayleigh distribution. The effects of aluminium that is about 30% of the stiffness and accounted for 4% or material of the system were neglectable. The effect can be observed when the stiffness of the bars was edited to 800GPa which is 4 times higher than the system which has been applied on.

The highest number of bar did not contributed to closest match to the natural frequency spacing that lead Rayleigh distribution. It was concluded to be the area and length of material variation which determine the natural frequency spacing distribution. When the length of the added material is small, even though higher number of bar, the bars has less effect on vibration each mode. This has been shown in result part where the closest match was from 30 bar model not the 50 bars model which is higher in number of bar.

The stiffness would make the response of steel plate of 500 mm in diameter and 5 mm in thickness random enough to generate Rayleigh distribution was unrealistic. The stiffness, even at 1200Gpa which close to diamond, still cannot produce enough randomness in response. The Statistical overlap factor also validated the result. They were getting higher overall as the sample from the result were closer to Rayleigh distribution but the system was not random enough where they are low or fluctuate between high and low value.

6.1 Future Work

The system need to be improved where the system should show a exponential distribution of natural frequency spacing while different number stiffness permutation can be simulated on the system. The tightening method could be improved by threading only half thickness of the plate instead of the bar. This is reducing the removal of material by 50% of original design. It, however need to be researched and tested if it would hold the bar firmly and the contacting surface still remain intact even at high frequency.

The excitation method can also be changed to shaker even though the impact hammer is proved to be a suitable where it is a quick and easy procedure to perform. This is to reduce any other uncertainty in measurement process. This could improve the result as the system itself is uncertainty already.

Analysis should cover higher frequency range as well as increasing number of both experimental and simulation sample to improve accuracy of result. This is when the shaker will be beneficial over impact hammer which only cover lower frequency range.

Reference

[1]N.F. Rieger, 1987, The quest for $\sqrt{k/m}$: Notes on the development of vibration analysis, Part I. genuine awakening, 4^{th} edition.

[2] Robin S. Langley, 2004, 'Mid and high-frequency vibration analysis of structure with uncertain properties', Eleventh International Congress on Sound and Vibration, St. Petersburg, Russia,

[3] Chen, P.C., Soroka, W.W., 1973, 'Impulse response of a dynamic system with statistical properties', Journal of Sound and Vibration **31**(3), pp. 309-314.

[4] Leissa, A.W., Narita, Y. 1980, 'Natural Frequencies of Simply Supported Circular Plates', Journal of Sound and Vibration, **70**(2), pp. 221-229.

[5] McWilliam, S., Ong, J. 2005, Fox, C.H.J., 'On the statistics of natural frequency splitting for rings with random mass imperfections', Journal of Sound and Vibration **279**(1-2), pp. 453–470.

[6] Fox, C.H.J. 1990, 'A Simple Theory for the Analysis and Correction of Frequency Splitting in Slightly Imperfect Rings', Journal of Sound and Vibration **142**(2), pp. 227-243.

[7] Duan, W.H., Wang, C.M., Wang, C.Y., 2008, 'Modification of Fundamental Vibration Modes of Circular Plates with Free Edges', Journal of Sound and Vibration, **317**(3-5), pp. 709-715.

[8] Lin, R. M., Lim, M. K. 1994, 'Natural Frequencies of Plates with Arbitrary concentrated Mass and Stiffness Modification', Journal of Sound and Vibration.

[9] Lucus, G.I. 2008, 'Vibrational Characteristics of Structures with Uncertainty', PhD. E thesis, University of New South Wales.

[10] Rao, S.S., Vibration of continuous system, John Wiley and Sons, 2007.

[11] Thomson, W.T., 1948, Mechanical Vibration, Prentice-Hall.

[12] Døssing, O. , 1988, Structural Tesing Part 1 Mechanical Mobility Measurement', Brüel & Kjær.

[13] Ewins, D.J., 1984, Modal Testing Theory and Practice , John Wiley & Sons.

[14] Eleanor, C., 2008, Discrete and Continuous Fourier Transforms, Chapman &Hall,

[15] Cooley, J. W., Tukey, J.W. , 1965, An algorithm for the machine calculation of complex Fourier series, Mathematic of Computation ,19.

[16] Irvine, T., 1999, The Steady-state Response of a Single-degree-of-freedom System Subjected to a Harmonic Force, Vibrationdata.com Publications.

[17] Rao, S.S., 2007, Vibration of continuous system, John Wiley and Sons.

[18] Liew, K.M., Wang, C.M., Xiang, Y. S., Kitipornchai, 1998,Vibration of Mindlin Plates, Elsevier.

[19] Leissa, A.W., 1993, Vibration of Plate, Acoustical Society of America.

[20] MathWorks, Rayleigh Distribution, The MathWorks Inc., USA.

[21] Smith, P.J., 1998, Into Statistic, 2nd edition, Springer.

[22] Papoulis, A., 1984, Probability, Random Variables, and Stochastic Processes, 2nd edition, McGraw-Hill, New York.

[23] Manohar, C. S., Keane, A. J., 1994, Statistics of Energy Flows in Spring-Coupled One-Dimensional Subsystems, Philosophical Transactions The Royal Society A, 346, pp.525-542.

[24] Døssing, O., 1988, Structural Tesing Part 1 Mechanical Mobility Measurement, Brüel & Kjær.

[25] Zhi-Fang, F., Jimin, H., 2001, Modal Analysis, Elsevier.

[26]Fox, C. H. J., Rourke, A. K.., McWilliam, S., 2001, 'Multi-ModeTrimming of Imperfect Rings', Journal of Sound and vibration, **248**(4), pp. 695-724.

Appendix

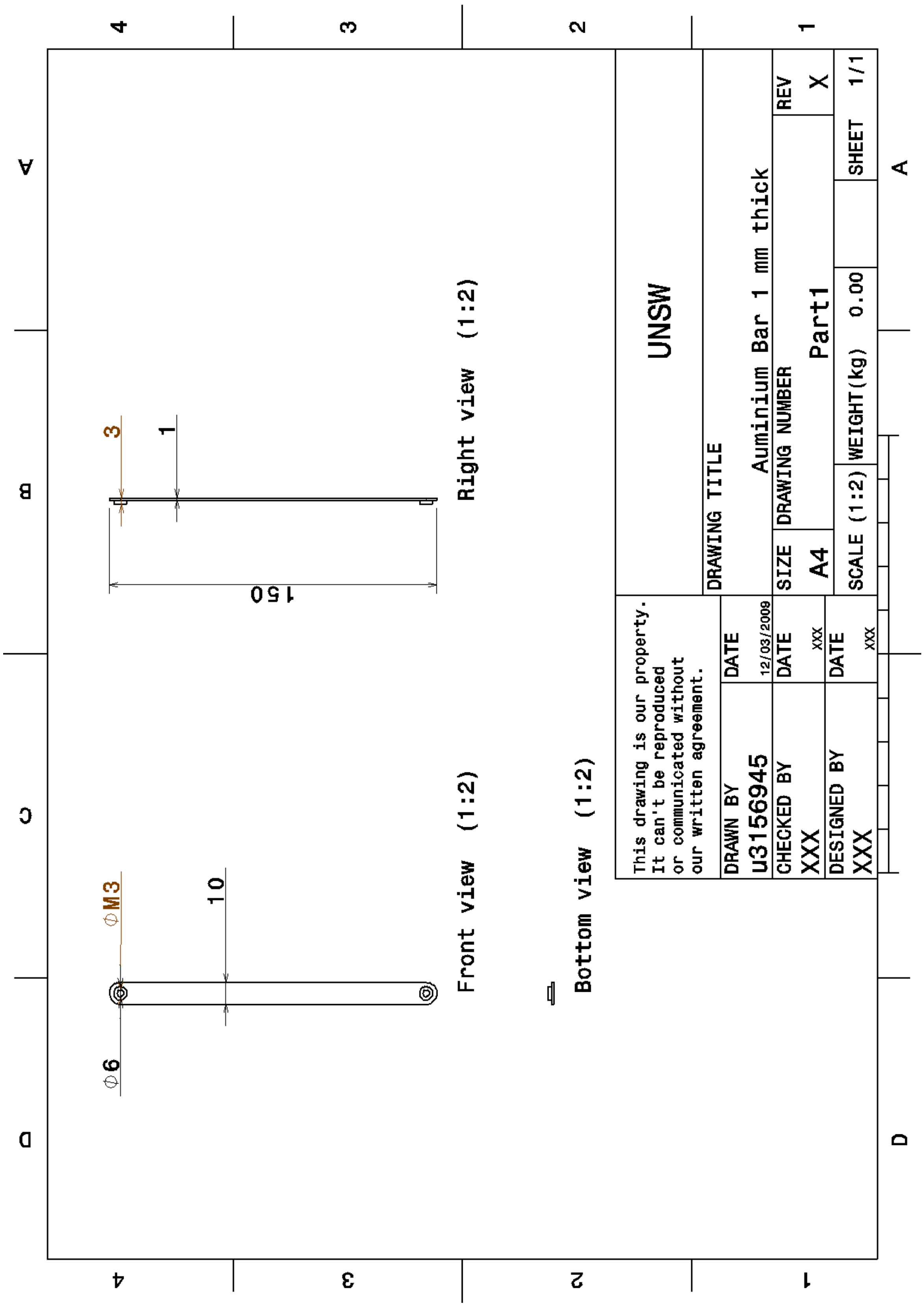

This drawing is our property.
It can't be reproduced
or communicated without
our written agreement.
DRAWING TITLE
Auminium Bar 1 mm thick
UNSW
DRAWN BY
u3156945
DATE
12/03/2009
CHECKED BY
XXX
DATE
XXX
DESIGNED BY
XXX
DATE
XXX
SIZE
A4
DRAWING NUMBER
Part1
REV
X
SCALE (1:2)
WEIGHT(kg) 0.00
SHEET 1/1
Front view (1:2)
Bottom view (1:2)
Right view (1:2)
ΦM3
Φ6
10
150
3
1

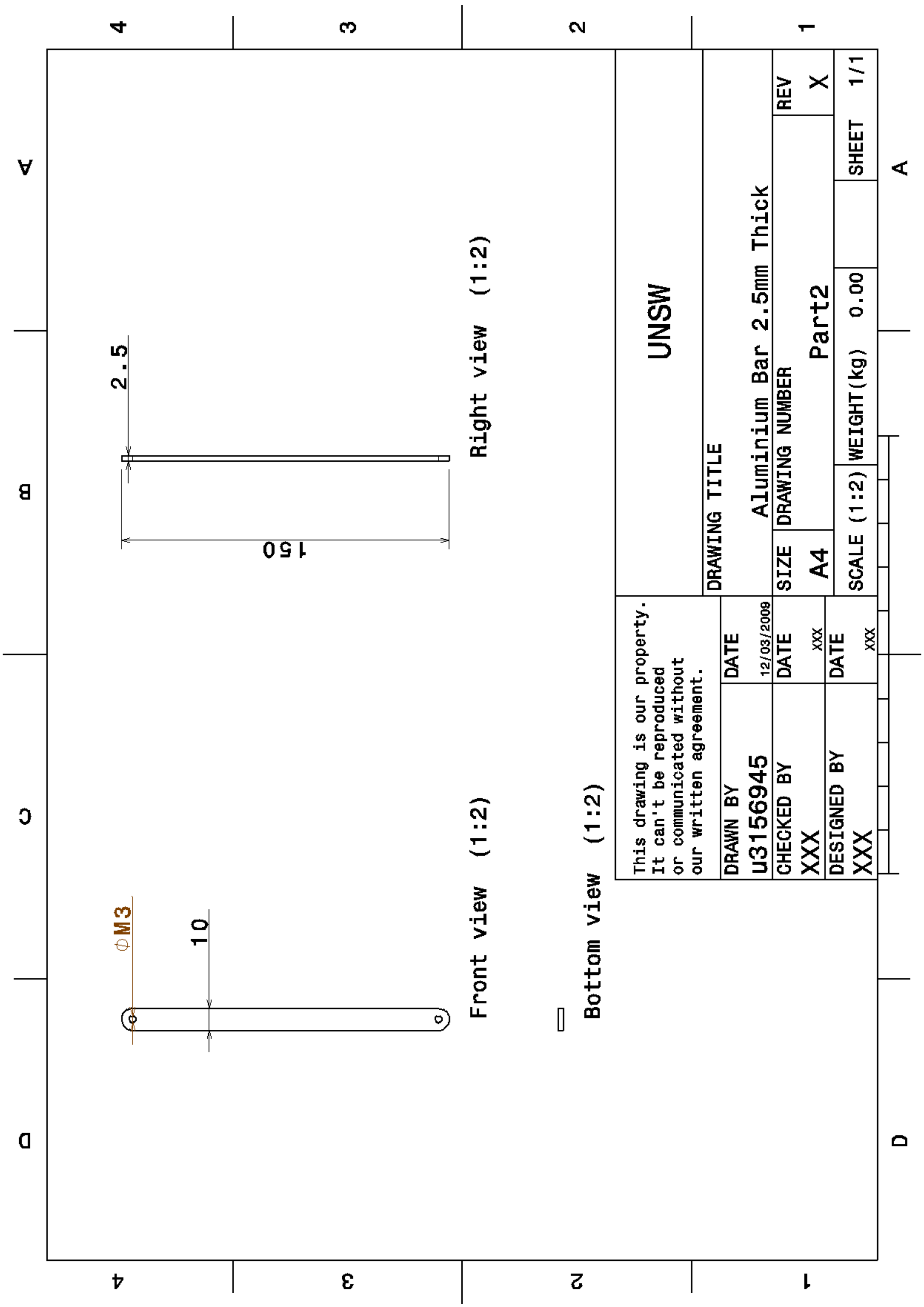

ΦM3
10
Front view (1:2)
Bottom view (1:2)
2.5
150
Right view (1:2)
This drawing is our property.
It can't be reproduced
or communicated without
our written agreement.
DRAWN BY
u3156945
DATE
12/03/2009
CHECKED BY
XXX
DATE
XXX
DESIGNED BY
XXX
DATE
XXX
UNSW
DRAWING TITLE
Aluminium Bar 2.5mm Thick
SIZE
A4
DRAWING NUMBER
Part2
REV
X
SCALE (1:2)
WEIGHT(kg) 0.00
SHEET 1/1

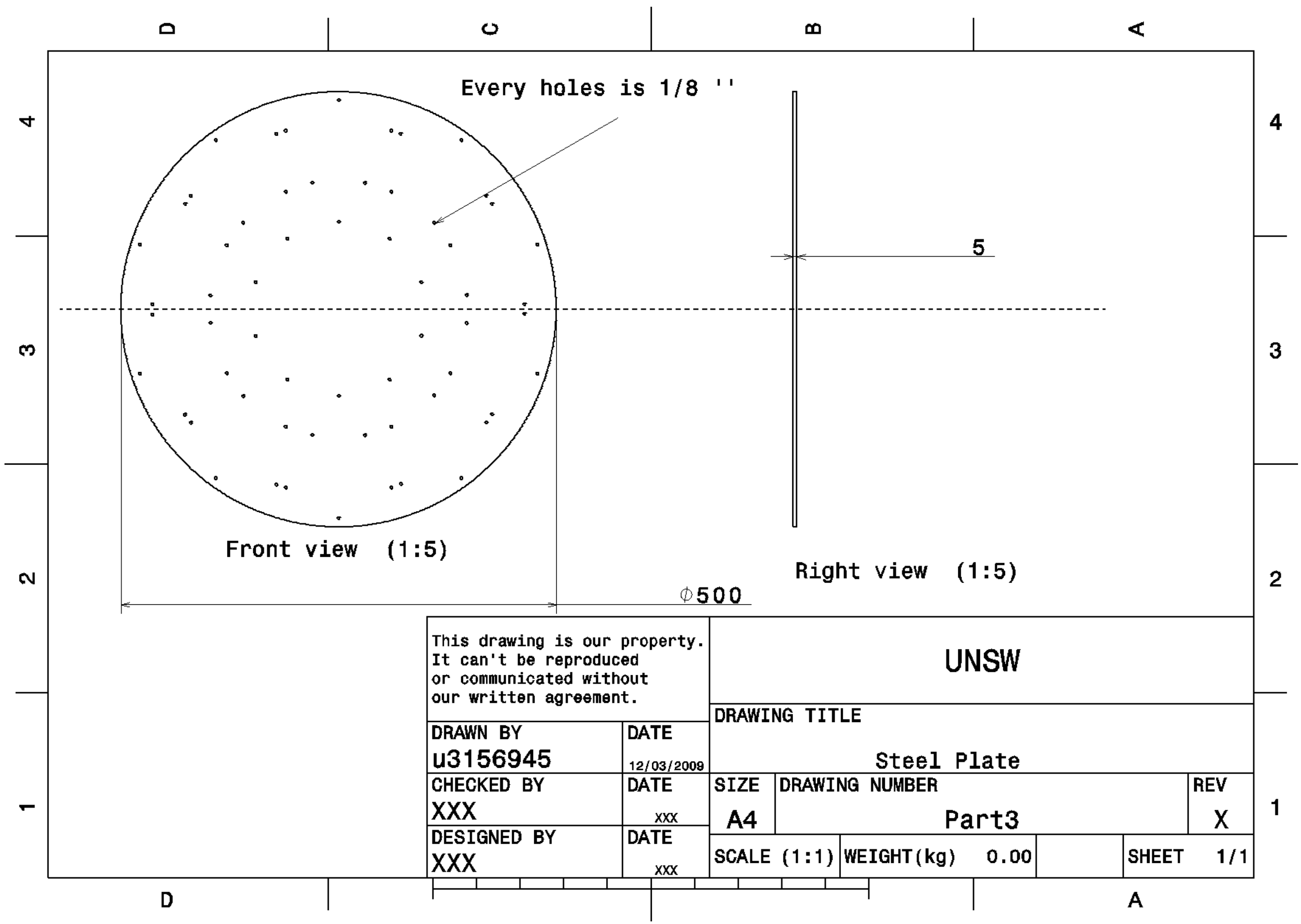
Every holes is 1/8 ''
5
Front view (1:5)
Right view (1:5)
Φ500
This drawing is our property.
It can't be reproduced
or communicated without
our written agreement.
UNSW
DRAWING TITLE
Steel Plate
DRAWN BY
u3156945
DATE
12/03/2009
CHECKED BY
XXX
DATE
XXX
DESIGNED BY
XXX
DATE
XXX
SIZE
A4
DRAWING NUMBER
Part3
REV
X
SCALE (1:1)
WEIGHT(kg) 0.00
SHEET 1/1